Studies on nanocrystalline Prussian blue and its mixed metal analogue for analytical application

THESIS

SUBMITTED FOR THE AWARD OF THE DEGREE OF

DOCTOR OF PHILOSOPHY

in

CHEMISTRY

by

Digvijay Panday

Under the supervision of

Prof. P. C. Pandey

DEPARTMENT OF CHEMISTRY
INDIAN INSTITUTE OF TECHNOLOGY
(BANARAS HINDU UNIVERSITY) VARANASI
VARANASI-221005, INDIA

Enrollment No. : 340519 **2016**

Dedicated

to

My Beloved Parents

Forwarded

Professor P.C.Pandey
Supervisor
Department of Chemistry
Indian Institute of Technology
(Banaras Hindu University)
Varanasi-221005, India

Professor R.B.Rastogi
Head
Department of Chemistry
Indian Institute of Technology
(Banaras Hindu University)
Varanasi-221005, India

Undertaking from the Candidate

I, **Digvijay Panday**, research scholar under the supervision of **Professor P.C.Pandey**, Department of Chemistry, Indian Institute of Technology (Banaras Hindu University), Varanasi give undertaking that the thesis entitled "**Studies on nanocrystalline Prussian blue and its mixed metal analogue for analytical application**" submitted by me for the degree of **Doctor of Philosophy** is a record of first-hand research work carried out by me during the period of study.

I avail myself to responsibility such as an act will be taken on the behalf of me, mistakes, errors of facts, and misinterpretation are of course entirely my own.

Date:

Place: Varanasi **(Digvijay Panday)**

Candidate's Declaration

I, **Digvijay Panday**, certify that the course work embodied in this Ph.D. thesis is my own bonafide work carried out by me under the supervision of **Professor P.C.Pandey**, Department of Chemistry, Indian Institute of Technology (Banaras Hindu University) Varanasi in a period of approximately 4 years 10 months from September, 2011 to July 2016) at Indian Institute of Technology (Banaras Hindu University), Varanasi. The matter embodied in this thesis has not been submitted for the award of any other degree/diploma.

I declare that I have faithfully acknowledged, given credit to and referred to the research workers wherever their works have been cited in the text and the body of the thesis. I further certify that I have not wilfully lifted up some other's works, paragraph, text, data, result etc. reported in the journals, books, magazines, reports, dissertations, thesis, *etc*., or available at websites and included them in this Ph.D. thesis and cited as my own work.

Date:

Place: (Digvijay Panday)

CERRTIFICATE FROM THE SUPERVISOR

This is to certify that the above statement made by the candidate is correct to the best of our knowledge.

(Professor P.C.Pandey)
Supervisor
Department of Chemistry
Indian Institute of Technology
(Banaras Hindu University) Varanasi
Varanasi-221005, India

(Professor R.B.Rastogi)
Head
Department of Chemistry
Indian Institute of Technology
(Banaras Hindu University) Varanasi
Varanasi-221005, India

Course work / Comprehensive Examination / Pre Submission Seminar Completion Certificate

This is to certify that Mr. Digvijay Panday, a bonafide research scholar of Department of Chemistry, Indian Institute of Technology (Banaras Hindu University), Varanasi has successfully completed the course work / comprehensive examination / pre-submission seminar requirement which is a part of his Ph.D. programme.

Date:
Place: Varanasi

Head
Department of Chemistry
Indian Institute of Chemistry
(Banaras Hindu University)
Varanasi

Copyright Transfer Certificate

Title of the Thesis : Studies on nanocrystalline Prussian blue and its mixed metal analogue for analytical application.

Candidate's Name : Digvijay Panday

Copyright Transfer

The undersigned hereby assigns to the Indian Institute of Technology (Banaras Hindu University), Varanasi all rights under copyright that may exist in and for the above thesis submitted for the award of the Ph.D. degree.

(Digvijay Panday)

Note: However, the author may reproduce or authorize others to reproduce material extracted verbatim from the thesis or derivative of the thesis for author's personal use provided that the source and Institute's / University's copyright notice are indicated.

Acknowledgement

First of all, I would like to thank to the Almighty God, who provide strength and the path to go ahead continuously. It is very difficult to mention all the inspiration, motivation in a short place because words are too weak to express feelings and sentiments.

I would like to express my gratitude to my supervisor **Professor P.C.Pandey** for his strong support, critical and invaluable guidance throughout the course of my candidature. I have learnt many things about research and various skills from him.

I am thankful to **Professor R.B.Rastogi**, Head of the Chemistry Department, for providing necessary facilities during the course of present research investigation.

I am also thankful to RPC members Prof. M.A.Quraishi, Prof. Y.C.Sharma and Prof. Rajeev Prakash (School of Material Science and Technology) for their invaluable inspiration and suggestions during the entire course of this research. I am also thankful to all the teaching and non-teaching staff of the Department of Chemistry for their assistance and help.

Moreover, I am thankful to all members of Prof. P.C.Pandey's group, Gunjan, Subhangi for sharing their knowledge and creating enjoyable lab environment both on and off the slopes. They will always be in my heart. Special thanks are due to all the past students from Prof. P.C.Pandey's lab, Dr.Arvind Prakash, Dr. Ashish Pandey and Richa Singh for the valuable discussions, help and for their awesome company.

I am grateful and thankful for all the support and encouragement from my batch mates and all of my friends in Indian Institute of Technology (Banaras Hindu University) and outside campus. There are too many to name everyone here but particular thanks to Deepak Gusain, Shivam Bajpai, Dr. Sudheer Malik, Dr. Ajit Singh (Department of Zoology, Banaras Hindu University), Dr. Piyoosh

Babele (Department of Biotechnology, Banaras Hindu University) for the essential support and wonderful friendship.

Furthermore, I would like to express my deepest gratitude to my parents for their continuous prayer, support and encouragement since birth which gave me to attain this esteemed pleasure of submitting this work for the degree of Ph.D. I am deeply beholden to my elder brother Dr. Deepak K. Pandey and sister in law Dr. Anita G. Pandey whose love, support and encouragement are the basis of my success. I am also very thankful to half part of my life, my wife Mrs. Seema Pandey who helped, encouraged, and motivated me whenever I need that.

I would also like to acknowledge the UGC and MHRD, Government of India, for providing me financial assistance (Junior Research Fellowship and Teaching assistantship). I would also like to thank the Indian Institute of Technology (Banaras Hindu University) for the opportunity given to me to pursue my further studies, as well as for the graduate scholarship given to me.

Last but not least, I wish to thank all my friends and foes and the persons whose names have not been included here for cooperation; directly and indirectly. They at all, if is there, this is inadvertent!

Contents

1 General Introduction 172

1.1 An overview on Metal Hexacyanoferrate (MHCFs)..... 172

1.1.1 Crystal structure of Prussian blue 173

1.1.2 Prussian blue Analogues (PBAs) 175

1.1.3 Synthesis of Prussian blue and its analogues 176

1.1.4 Properties of Prussian blue and its analogues 182

1.1.5 Properties of Mixed metal hexacyanoferrates (MHCFs) 194

1.2 Prussian blue and its mixed metal analogue in analytical applications . 197

1.2.1 Electrochemical applications of Prussian blue and its mixed metal analogues..... 198

1.2.2 Artificial Peroxidase like activity of nanomaterial: Special reference to Prussian blue and its analogues in application of H_2O_2 207

1.3 Challenges in Prussian blue and its mixed metal analogues related work... 210

1.4 Origin of the present research work..... 211

1.5 Objective of the present research work..... 212

1.6 Work plan for the present research work 215

2 THF and H_2O_2 mediated synthesis of nanocrystalline PBNPs and its analytical applications..... **Error! Bookmark not defined.**

2.1 Introduction..... **Error! Bookmark not defined.**

2.2 Experimental ..... **Error! Bookmark not defined.**

2.2.1 Material and Methods ..... **Error! Bookmark not defined.**

2.2.2 THF and H_2O_2 mediated synthesis of nanocrystalline Prussian blue nanoparticles ..... **Error! Bookmark not defined.**

2.2.3 Measurement and characterization.... **Error! Bookmark not defined.**

2.2.4 Peroxidase like catalytic activity of Prussian blue nanoparticles **Error! Bookmark not defined.**

2.2.5 Preparation of modified graphite paste electrode**Error! Bookmark not defined.**

2.3 Results ..... **Error! Bookmark not defined.**

2.3.1 THF and H_2O_2 mediated synthesis of nanocrystalline PBNPs ..**Error! Bookmark not defined.**

2.3.2 Electrochemical characterization of as synthesized PBNPs .....**Error! Bookmark not defined.**

2.3.3 Peroxidase like activity of PBNPs made through THF and H_2O_2 **Error! Bookmark not defined.**

2.3.4 Electrocatalytic reduction of H_2O_2 on the PBNPs modified electrode . ..... **Error! Bookmark not defined.**

2.4 Discussion ..... **Error! Bookmark not defined.**

2.4.1 Optimization of THF and H_2O_2 mediated synthesis of nanocrystalline PBNPs ..... **Error! Bookmark not defined.**

2.4.2 Characterization of THF and H_2O_2 mediated synthesized nanocrystalline PBNPs..... **Error! Bookmark not defined.**

2.4.3 Electrochemical analysis of THF and H_2O_2 mediated synthesized PBNPs ..... **Error! Bookmark not defined.**

2.4.4 Peroxidase like activity of PBNPs .... **Error! Bookmark not defined.**

2.4.5 Electrocatalytic reduction of hydrogen peroxide over THF, H_2O_2 mediated synthesized PBNPs modified graphite electrode .....**Error! Bookmark not defined.**

2.5 Stability and Reproducibility ..... **Error! Bookmark not defined.**

3 THF and H_2O_2 mediated synthesis of nanocrystalline Ni-Fe HCFs and its analytical applications ..... **Error! Bookmark not defined.**

3.1 Introduction ..... **Error! Bookmark not defined.**

3.2 Experimental ..... **Error! Bookmark not defined.**

3.2.1 Material and Methods ..... **Error! Bookmark not defined.**

3.2.2 Synthesis of nanocrystalline Ni-Fe hexacyanoferrates (Ni-Fe HCFs).. ..... **Error! Bookmark not defined.**

3.2.3 Structural characterization of Ni-Fe hexacyanoferrates (1:5).... **Error! Bookmark not defined.**

3.2.4 Peroxidase mimetic activity measurement of Ni-Fe HCFs (1:5) **Error! Bookmark not defined.**

3.2.5 Preparation of modified graphite paste electrode **Error! Bookmark not defined.**

3.2.6 Electrochemical Measurements ..... **Error! Bookmark not defined.**

3.3 Results ..... **Error! Bookmark not defined.**

3.3.1 Synthesis of nanocrystalline Ni-Fe HCFe mediated through $K_3[Fe(CN)_6]$, THF, H_2O_2 and $NiSO_4$ **Error! Bookmark not defined.**

3.3.2 Characterization of Ni-Fe HCFs synthesized through THF, H_2O_2 and $NiSO_4$ (1:5) ..... **Error! Bookmark not defined.**

3.3.3 Peroxidase like activity of Ni-Fe HCFs nanoparticles (1:5) ..... **Error! Bookmark not defined.**

3.3.4 Electrocatalytic oxidation of hydrazine over Ni-Fe HCFs (1:5) nanoparticles modified electrode ..... **Error! Bookmark not defined.**

3.4 Discussion ..... **Error! Bookmark not defined.**

3.4.1 THF and H_2O_2 mediated synthesis of nanocrystalline Ni-Fe hexacyanoferrates..... **Error! Bookmark not defined.**

3.4.2 Structural analysis of Ni-Fe HCFs nanoparticles (1:5) ..... **Error! Bookmark not defined.**

3.4.3 Electrochemical analysis of Ni-Fe hexacyanoferrates ..... **Error! Bookmark not defined.**

3.4.4 Peroxidase mimetic behaviour of Ni-Fe hexacyanoferrates (1:5) **Error! Bookmark not defined.**

3.4.5 Electrochemical sensing of hydrazine over Ni-Fe hexacyanoferrates (1:5) modified electrode ..... **Error! Bookmark not defined.**

4 Polyethylenimine mediated synthesis of Prussian blue nanoparticles and cooperative self assembly of gold nanoparticles on Polycationic surface **Error! Bookmark not defined.**

4.1 Introduction ..... **Error! Bookmark not defined.**

4.2 Experimental ..... **Error! Bookmark not defined.**

4.2.1 Material and Methods ..... **Error! Bookmark not defined.**

4.2.2 Synthesis of cationic polymer coated nanocrystalline PBNPs and AuNPs assembled PBNPs ..... **Error! Bookmark not defined.**

4.2.3 Measurement and characterization.... **Error! Bookmark not defined.**

4.2.4 Electrochemical measurements and preparation of modified graphite paste electrode ..... **Error! Bookmark not defined.**

4.2.5 Peroxidase like activity of PBNPs and AuNPs assembled PBNPs **Error! Bookmark not defined.**

4.3 Results ..... **Error! Bookmark not defined.**

4.3.1 PEI mediated synthesis of nanocrystalline PBNPs and AuNPs assembled PBNPs ..... **Error! Bookmark not defined.**

4.3.2 Structural characterization ..... **Error! Bookmark not defined.**

4.3.3 Electrochemical characterization of PEI mediated synthesized PBNPs ..... **Error! Bookmark not defined.**

4.3.4 Peroxidase mimetic activity of PBNPs and AuNPs assembled PBNPs ..... **Error! Bookmark not defined.**

4.3.5 Electrocatalytic reduction and oxidation of H_2O_2 over PBNPs and AuNPs assembled PBNPs modified electrode**Error! Bookmark not defined.**

4.3.6 Magnetic measurement of PBNPs and AuNPs assembled PBNPs **Error! Bookmark not defined.**

4.4 Discussion ..... **Error! Bookmark not defined.**

4.4.1 PEI mediated synthesis of nanocrystalline PBNPs**Error! Bookmark not defined.**

4.4.2 Characterization of cationic polymer coated PBNPs and AuNPs assembled PBNPs ..... **Error! Bookmark not defined.**

4.4.3 Electrochemistry and catalytic activity of PBNPs and AuNPs assembled PBNPs modified electrode**Error! Bookmark not defined.**

4.4.4 Homogeneous catalysis of PBNPs and AuNPs assembled PBNPs **Error! Bookmark not defined.**

4.4.5 PBNPs and AuNPs assembled PBNPs mediated reduction of H_2O_2 .... **Error! Bookmark not defined.**

4.4.6 PBNPs and AuNPs assembled PBNPs mediated oxidation of H_2O_2 .... **Error! Bookmark not defined.**

4.4.7 Magnetic properties of cationic polymer coated PBNPs and AuNPs assembled PBNPs ..... **Error! Bookmark not defined.**

5 PEI mediated synthesis of Cu-Fe HCFs and Ni-Fe HCFs nanoparticles and their analytical applications..... **Error! Bookmark not defined.**

5.1 Introduction ..... **Error! Bookmark not defined.**

5.2 Experimental ..... **Error! Bookmark not defined.**

5.2.1 Material and Methods ..... **Error! Bookmark not defined.**

5.2.2 Synthesis of Cu-Fe hexacyanoferrates and Cu-hexacyanoferrates **Error! Bookmark not defined.**

5.2.3 Synthesis of Ni-Fe hexacyanoferrates and Ni-hexacyanoferrates **Error! Bookmark not defined.**

5.2.4 Structural characterization of mixed metal hexacyanoferrates..**Error! Bookmark not defined.**

5.2.5 Peroxidase mimetic activity of mixed metal hexacyanoferrates**Error! Bookmark not defined.**

5.2.6 Fabrication of modified graphite paste electrode**Error! Bookmark not defined.**

5.2.7 Electrochemical Measurements ..... **Error! Bookmark not defined.**

5.3 Results ..... **Error! Bookmark not defined.**

5.3.1 PEI mediated synthesis of nanocrystalline mixed metal hexacyanoferrates..... **Error! Bookmark not defined.**

5.3.2 Structural characterization ..... **Error! Bookmark not defined.**

5.3.3 Electrochemical characterization ..... **Error! Bookmark not defined.**

5.3.4 Peroxidase mimetic activity of as synthesized Cu-Fe HCFs (1:1) and Ni-Fe HCFs (1:5) ..... **Error! Bookmark not defined.**

5.3.5 Electrocatalytic analysis of dopamine, hydrazine and H_2O_2 over Cu-Fe HCFs (1:1) and Ni-Fe HCFs (1:5) modified electrode .....**Error! Bookmark not defined.**

5.4 Discussion ..... **Error! Bookmark not defined.**

5.4.1 PEI mediated synthesis of nanocrystalline Cu-Fe HCF and Ni-Fe HCFs ..... **Error! Bookmark not defined.**

5.4.2 Characterization of Cu-Fe HCFs (1:1) and Ni-Fe HCFs (1:5)...**Error! Bookmark not defined.**

5.4.3 Electrochemical behaviour of mixed metal analogue .....**Error! Bookmark not defined.**

5.4.4 Peroxidase mimetic activity of Cu-Fe HCFs (1:1) and Ni-Fe HCFs (1:5) ..... **Error! Bookmark not defined.**

5.4.5 Electrocatalytic oxidation of dopamine, hydrazine and hydrogen peroxide over Cu-Fe HCFs (1:1) and Ni-Fe HCFs (1:5) .....**Error! Bookmark not defined.**

5.4.6 Stability and Reproducibility ..... **Error! Bookmark not defined.**

Summary……...……167

Future Projection…….…..170

References…….171

List of Publication……..……...205

List of Figures

Figure.1.1. 3D structure of soluble PB (A) and insoluble PB (B), Fe(II) yellow, Fe (III) brown, K magenta, C grey, O red [(Shokouhimehr *et al.* 2010)]. 174

Figure.1.2. Cyclic voltammogram of a PB modified electrode showing oxidation and reduction peak [(Ricci and Palleschi 2005)] 184

Figure.2.1. Schematic presentation of synthesis of PBNPs from optimum concentration of $K_3[Fe(CN)_6]$, THF and H_2O_2. ..... **Error! Bookmark not defined.**

Figure.2.2. UV–Vis spectra of systems containing constant concentration of THF (1.2 M) and $K_3[Fe(CN)_6]$ (25 mM) and the varying concentration of H_2O_2 (from 0.003 M to 1.40 M). The corresponding vial visual photographs are shown in the inset of the respective systems. ..... **Error! Bookmark not defined.**

Figure.2.3. Systems containing constant concentration of $K_3[Fe(CN)_6]$ (25 mM): and H_2O_2 (0.70 M): and varying concentration of THF (from 0.15 M to 4.5 M). The corresponding vial visual photographs are shown in the inset of the respective systems. ..... **Error! Bookmark not defined.**

Figure.2.4. Systems containing constant concentration of THF (1.2 M) and H_2O_2 (0.7 M): and varying concentration of $K_3[Fe(CN)_6]$ (from 3 mM to 45 mM): The corresponding vial visual photographs are shown in the inset of the respective systems. ..... **Error! Bookmark not defined.**

Figure.2.5. FT-IR spectra of THF and H_2O_2 mediated synthesized PBNPs..... **Error! Bookmark not defined.**

Figure.2.6. XRD pattern of THF and H_2O_2 mediated synthesized PBNPs. ..... **Error! Bookmark not defined.**

Figure.2.7. EDS spectra of THF and H_2O_2 mediated synthesized of PBNPs. ..... **Error! Bookmark not defined.**

Figure.2.8. TEM image of THF and H_2O_2 mediated synthesized of PBNPs. ..... **Error! Bookmark not defined.**

Figure.2.9. (A) Cyclic voltammograms of THF and H_2O_2 mediated synthesized PBNPs in 0.1 M KNO_3 at various scan rates between 0.01 V s^{-1} and 0.3 V s^{-1}. (B) A typical voltammogram of THF and H_2O_2 mediated synthesized PBNPs at scan rate 0.005 V s^{-1}. (C) The plots of peak current density vs. scan rate for PBNPs. (D) the plots of peak current density *vs.* square root of scan rate for PBNPs... **Error! Bookmark not defined.**

Figure.2.10. Colour conversion of o-dianisidine and H_2O_2 in the presence of metal hexacyanoferrates. ..... **Error! Bookmark not defined.**

Figure.2.11. Time dependent absorbance changes at 430 nm in the presence of different concentrations of H_2O_2 (from 0.05 mM to 14 mM and fixed concentration of o-dianisidine (50 μM) catalyzed by PBNPs.... **Error! Bookmark not defined.**

Figure.2.12. Kinetic analysis of PBNPs with H_2O_2 as substrate. **Error! Bookmark not defined.**

Figure.2.13. Cyclic voltammograms of PBNPs modified electrode in the absence (1) and the presence (2) of 1 mM H_2O_2 in 0.1 M phosphate buffer pH=7.0 containing 0.5 M KCl..... **Error! Bookmark not defined.**

Figure.2.14. Amperometric response of PBNPs modified electrode on the addition of varying concentrations of H_2O_2 between 0.01 mM and 5 mM; operating potential, 0.0 V; 0.1 M phosphate buffer (pH=7.0) containing 0.5 M KCl as supporting electrolyte, The inset (B) shows calibration plots for PBNPs..... **Error! Bookmark not defined.**

Figure.3.1. Schematic presentation of Ni-Fe hexacyanoferrates formation from THF, H_2O_2 and $K_3[Fe(CN)_6]$ and $NiSO_4$..... **Error! Bookmark not defined.**

Figure.3. 2. Effect of THF on the formation of Ni–Fe HCF at constant molar ratio of Ni and Fe (1:5) and H_2O_2. ..... **Error! Bookmark not defined.**

Figure.3. 3. Effect of H_2O_2 on the formation of Ni–Fe HCF at constant molar ratio of Ni and Fe (1:5) and THF..... **Error! Bookmark not defined.**

Figure.3.4. AFM image of THF and H_2O_2 mediated synthesized Ni–Fe HCF (1:5). .... **Error! Bookmark not defined.**

Figure.3.5. FT-IR spectra of THF and H_2O_2 mediated synthesized Ni–Fe HCF (1:5). . **Error! Bookmark not defined.**

Figure.3.6. XRD analysis of THF and H_2O_2 mediated synthesized Ni–Fe HCF (1:5). . **Error! Bookmark not defined.**

Figure.3.7. SEM image of THF and H_2O_2 mediated synthesized Ni–Fe HCF (1:5). .... **Error! Bookmark not defined.**

Figure.3.8. TEM image of Ni–Fe HCF (1:5), inset shows the respective size distribution. **Error! Bookmark not defined.**

Figure.3.9. Energy dispersive spectroscopy of THF and H_2O_2 mediated synthesized Ni–Fe HCF (1:5). Inset shows the weight %age of EDS analysis. **Error! Bookmark not defined.**

Figure.3.10. Cyclic voltammetric response of THF and H_2O_2 mediated synthesized Ni–FeHCF modified carbon paste electrodes in 0.1 M KNO_3 at a scan rate of 0.01 V s^{-1} made at different Ni:Fe molar ratio: [A] only PBNPs; [B] Ni– Fe HCF (1:20); [C] Ni–Fe HCF (1:10); [D] Ni–Fe HCF (1:5); [E] Ni–Fe HCF (1:3); [F] Ni–Fe HCF (1:2). ..... **Error! Bookmark not defined.**

Figure.3.11. Cyclic voltammetric response of THF and H_2O_2 mediated synthesized Ni–FeHCF modified carbon paste electrodes in 0.1 M KNO_3 at different scan rate of 0.01, 0.02, 0.035, 0.05, 0.07, 0.10, 0.15, 0.20, 0.25, 0.35 V s^{-1} made at different Ni:Fe molar ratio: [A] only PBNPs; [B] Ni– Fe HCF (1:20); [C] Ni–Fe HCF (1:10); [D] Ni–Fe HCF (1:5); [E] Ni–Fe HCF (1:3); [F] Ni–Fe HCF (1:2). ..... **Error! Bookmark not defined.**

Figure.3.12. (A) Time dependence absorbance changes at 430 nm in the presence of different concentrations (0.05, 0.10, 0.21, 0.43, 0.86, 1.70, 3.40, 6.80 and 13.60 mM) of H_2O_2 and at fixed concentration of o-dianisidine (50 μM) catalysed by Ni–Fe HCF (1:5), and (B) kinetic analysis of Ni–Fe HCF (1:5) with H_2O_2 as substrate. ..... **Error! Bookmark not defined.**

Figure.3.13. Cyclic voltammogram of Ni–Fe HCF (1:5) in the absence (1) and presence (2) of 1 mM hydrazine recorded in 0.1 M $NaNO_3$, pH=7.0 at scan rate of 0.01 V s^{-1}. ..... **Error! Bookmark not defined.**

Figure.3.14. Amperometric response of Ni–Fe HCF (1:5) modified electrode on the addition of varying concentration of hydrazine between 0.01 M to 5 mM; operating potential 0.3 V; 0.1 M $NaNO_3$ was the supporting electrolyte..... **Error! Bookmark not defined.**

Figure.3.15. Calibration curve for hydrazine analysis..... **Error! Bookmark not defined.**

Figure.4.1. UV-Vis spectra of showing requirement of optimum concentration of both $K_3[Fe(CN)_6]$ and PEI in acidic medium for the synthesis of PBNPs. ..... **Error! Bookmark not defined.**

Figure.4.2. UV-Vis spectra of system containing constant concentration of $K_3[Fe(CN)_6]$ (25 mM) and the varying concentration of PEI (A) 10 mg/ml (B) 20 mg/ml) (C) 30 mg/ml and (D) 40 mg/ml. ..... **Error! Bookmark not defined.**

Figure.4. 3. UV-Vis spectra of system containing constant concentration of PEI (20 mg/ml) and the varying concentrations of $K_3[Fe(CN)_6]$ (A) 10 mM (B) 25 mM (C) 35 mM and (D) 50 mM respectively..... **Error! Bookmark not defined.**

Figure.4. 4. Schematic presentation of cationic polymer coating and formation of PBNPs (A), AuNPs (B) and AuNPs assembled on cationic surface of PBNPs (C). **Error! Bookmark not defined.**

Figure.4. 5. XRD pattern of PBNPs (A) and AuNPs assembled PBNPs (B). ..... **Error! Bookmark not defined.**

Figure.4. 6. TEM image of PBNPs (A) and AuNPs assembled PBNPs (B). Inset to the figure shows selected area electron diffraction pattern. **Error! Bookmark not defined.**

Figure.4. 7. Cyclic voltammograms of PBNPs (A) and AuNPs assembled PBNPs (B) electrode in 0.1 M KNO_3 at the scan rate of: 10, 20, 35, 50, 70, 100, 150, 200, 250, and 300 mV s^{-1} consecutively..... **Error! Bookmark not defined.**

Figure.4. 8. The plot of anodic and cathodic current density *vs.* scan rate (A and C) and square root of scan rate (B and D) for PBNPs (A and C) and AuNPs assembled PBNPs (B and D) respectively. ..... **Error! Bookmark not defined.**

Figure.4.9. Time dependent absorbance changes at 430 nm in the presence of different concentrations of H_2O_2 (from 0.18 mM to 25 mM) and fixed concentration of o-dianisidine (50 μM) catalyzed by PBNPs (A) and Kinetic analysis of PBNPs (B)..... **Error! Bookmark not defined.**

Figure.4.10. Time dependent absorbance changes at 430 nm in the presence of different concentrations of H_2O_2 (from 0.18 mM to 25 mM) and fixed concentration of o-dianisidine (50 μM) catalyzed by AuNPs assembled PBNPs (A), and Kinetic analysis of AuNPs assembled PBNPs (B). .. **Error! Bookmark not defined.**

Figure.4.11. Cyclic voltammograms of PBNPs (A) and AuNPs assembled PBNPs (B) in absence (1) and the presence (2) of 1 mM H_2O_2 at the scan rate of 0.01 V s^{-1} in 0.1 M phosphate buffer (pH=7.0) containing 0.5 M KCl.**Error! Bookmark not defined.**

Figure.4.12. Amperometric response of PBNPs (1) and AuNPs assembled PBNPs (2) modified electrodes at 0.2 V *vs.* Ag|AgCl on the addition of varying concentrations of H_2O_2 in 0.1 phosphate buffer containing 0.5 M KCl....**Error! Bookmark not defined.**

Figure.4.13. Calibration curve of H_2O_2 reduction obtained from amperograms of PBNPs (1) and AuNPs assembled PBNPs (2)..... **Error! Bookmark not defined.**

Figure.4.14. Chronoamperograms for PBNPs (A) and AuNPs assembled PBNPs (B) modified electrode in the absence (black curve) and in the presence (red curve) of 1 mM H_2O_2. The step potential was -0.05 V *vs.* Ag|AgCl. Inset: corresponding plots of I_{cat}/I_L vs. $t^{1/2}$ in 0.1 M phosphate buffer containing 0.5 M KCl as supporting electrolyte..... **Error! Bookmark not defined.**

Figure.4.15. Cyclic voltammograms of PBNPs (A) and AuNPs assemble PBNPs (B) in absence (1) and presence (2) of 1 mM H_2O_2 at the scan rate of 0.01 V s^{-1} in 0.1 M phosphate buffer (pH=7.0) containing 0.5 M KCl.**Error! Bookmark not defined.**

Figure.4.16. Amperometric response of PBNPs (1) and AuNPs-PBNPs (2) modified electrodes at 0.6 V *vs.* Ag|AgCl on the addition of varying concentrations of H_2O_2 in 0.1 phosphate buffer (pH=7.0) containing 0.5 M KCl. .....**Error! Bookmark not defined.**

Figure.4. 17. Calibration curve of oxidation of H_2O_2 obtained from amperograms of PBNPs (1) and AuNPs assembled PBNPs (2).**Error! Bookmark not defined.**

Figure.4.18. Normalized zero-field-cooled (ZFC) and field-cooled (FC) magnetizations of PBNPs at different applied field (H): A=25, B=50 and C=100 Oe; (D) Magnetization hysteresis loops at 2 K, 5 K, and 10 K respectively (D). ...**Error! Bookmark not defined.**

Figure.4.19. Normalized zero-field-cooled (ZFC) and field-cooled (FC) magnetizations of PBNPs (A) and AuNPs assembled PBNPs (B) at 100 Oe applied field (H). **Error! Bookmark not defined.**

Figure.5.1. Schematic presentation of PEI mediated synthesis of Cu-Fe hexacyanoferrates and Ni-Fe hexacyanoferrates nanoparticles. **Error! Bookmark not defined.**

Figure.5. 2. UV-Vis spectroscopy of Cu-Fe HCFs (1:1) and Ni-Fe HCFs (1:5) made through $K_4[Fe(CN)_6]$ and $K_3[Fe(CN)_6]$ at 60 °C in 3 hours.**Error! Bookmark not defined.**

Figure.5. 3. Cyclic voltammogram of (A) Cu-Fe HCFs (1:1) (B) Ni-Fe HCFs (1:5) [made through $K_4Fe(CN)_6$ and PEI at 60 °C); and (C) Cu-Fe HCFs (1:1) (D) Ni-Fe HCFs (1:5) [made through $K_3Fe(CN)_6$ and PEI at 60 °C].**Error! Bookmark not defined.**

Figure.5. 4. UV-Vis spectroscopy of (A) Cu-Fe HCFs (1:1) (B) Ni-Fe HCFs (1:5) made at (1) room temperature (2) 90 °C and (3) 60 °C. . **Error! Bookmark not defined.**

Figure.5. 5. Cyclic voltammetry of (A) to (C) for Cu-Fe HCFs (1:1) and (D) to (F) for Ni-Fe HCFs (1:5) [synthesized at room temperature, 60 °C and 90 °C] in 0.1 M KNO_3 as electrolyte..... **Error! Bookmark not defined.**

Figure.5. 6. Cyclic voltammogram of (A) Cu-Fe HCFs (1:1) and (B) Ni-Fe HCFs (1:5) made without PEI at scan rate of 0.01 V s^{-1} in 0.1 M KNO_3 as a electrolyte; UV-Vis spectroscopy (C) of the (1) Ni-Fe HCFs (1:5) and (2) Cu-Fe HCFs (1:1) synthesized without PEI in 24 hours..... **Error! Bookmark not defined.**

Figure.5. 7. FT-IR spectra of (A) Cu-Fe HCFs (1:1) and (B) Ni-Fe HCFs (1:5).....**Error! Bookmark not defined.**

Figure.5. 8. XRD analysis of (A) Cu-Fe HCFs (1:1) and (B) Ni-Fe HCFs (1:5).....**Error! Bookmark not defined.**

Figure.5. 9. TEM image of (A) Cu-Fe HCFs (1:1) and (B) Ni-Fe HCFs (1:5); inset to the each figure shows the SAED pattern of respective metal hexacyanoferrates; SEM image of (C) Cu-Fe HCFs (1:1) and (D) Ni-Fe HCFs (1:5). .....**Error! Bookmark not defined.**

Figure.5. 10. EDS spectra of (A) Cu-Fe HCFs (1:1) and (B) Ni-Fe HCFs (1:5). .....**Error! Bookmark not defined.**

Figure.5. 11. Cyclic voltammetry response of Cu-Fe HCFs modified graphite paste electrode in 0.1 M KNO_3 at scan rate of 0.01 V s^{-1} made at different Cu:Fe molar ratio [A] PBNPs; [B] Cu:Fe (1:10); [C] Cu:Fe (1:5); [D] Cu:Fe (1:3); [E] Cu:Fe (1:2); [F] Cu:Fe (1:1); (G) Cu:Fe (2:1); [H] Cu:Fe (3:1); and [I] CuHCFs .....**Error! Bookmark not defined.**

Figure.5. 12. Cyclic voltammetry response of Cu-Fe HCFs modified graphite paste electrode in 0.1 M KNO_3 at scan rate of 0.01, 0.02, 0.035, 0.05, 0.07, 0.10, 0.15, 0.20, 0.25, 0.30 V s^{-1} made at different Cu:Fe molar ratio [A] PBNPs; [B] Cu:Fe (1:10); [C] Cu:Fe (1:5); [D] Cu:Fe (1:3); [E] Cu:Fe (1:2); [F] Cu:Fe (1:1); (G) Cu:Fe (2:1); [H] Cu:Fe (3:1) and [I] CuHCFs.**Error! Bookmark not defined.**

Figure.5. 13. The plots of peak current density *vs*. scan rate for Cu-Fe HCFs made at different molar ratio of Cu:Fe [A] 1:10 [B] 1:5 [C] 1:3 and [D] 1:2.**Error! Bookmark not defined.**

Figure.5. 14. Cyclic voltammetry response of Ni-Fe HCFs modified graphite paste electrode in 0.1 M KNO_3 at scan rate of 0.01 V s^{-1} made at different Ni:Fe molar ratio [A] only PBNPs; [B] Ni:Fe (1:20); [C] Ni:Fe (1:10); [D] Ni:Fe (1:5); [E] Ni:Fe (1:3); [F] Ni:Fe (1:2); [G] NiHCFs. ..... **Error! Bookmark not defined.**

Figure.5. 15. Cyclic voltammetry response of Ni-Fe HCFs modified graphite paste electrode in 0.1 M KNO_3 at varying scan rate of 0.01, 0.02, 0.035, 0.05, 0.07, 0.10, 0.15, 0.20, 0.25, 0.30 V s^{-1} made at different Ni:Fe molar ratio [A] PBNPs; [B] Ni:Fe (1:20); [C] Ni:Fe (1:10); [D] Ni:Fe (1:5); [E] Ni:Fe (1:3); [F] Ni:Fe (1:2); and [G] NiHCFs. ..... **Error! Bookmark not defined.**

Figure.5. 16. The plots of peak current density *vs*. scan rate for Ni-Fe HCFs made at different molar ratio of Ni:Fe [A] PB [B] 1:20 [C] 1:20 [D] 1:10 [E] 1:5, [F] 1:3 and [1:2]. ..... **Error! Bookmark not defined.**

Figure.5. 17. Cyclic voltammetry of (A) to (C) for Cu-Fe HCFs (1:1) and (D) to (F) for Ni-Fe HCFs (1:5) under different pH=4.0 (phthalate buffer), pH=7.0 (phosphate buffer) and pH=9.0 (borate buffer) containing 0.5 M KCl.**Error! Bookmark not defined.**

Figure.5. 18. Time dependent absorbance changes at 430 nm in the presence of different concentration (25, 18, 13, 6.5, 3.25, 1.5, 0.75, 0.75, 0.37 and 0.18 mM) of H_2O_2 and fixed concentration of o-dianisidine (50 μM) catalyzed by (A) Cu-Fe HCFs (1:1) and (B) Ni-Fe HCFs (1:5); and kinetic analysis of (C) Cu:Fe HCFs (1:1) and (D) Ni-Fe HCFs (1:5) with H_2O_2 as substrate.**Error! Bookmark not defined.**

Figure.5. 19. Cyclic voltammogram of (A) Cu-Fe HCFs (1:1) and (B) Ni-Fe HCFs (1:5) in the absence (1) and presence of (2) 2 mM and (3) 5 mM dopamine recorded in 0.1 M phosphate buffer containing 0.5 M KCl, (pH=7.0) at scan rate of 0.01 V s-1; (B) amperometric response of (C) Cu-Fe HCFs (1:1) and (D) Ni-Fe HCFs (1:5) modified graphite paste electrode on the addition of varying concentration of dopamine between 0.01 μM to 5 mM; operating potential 0.2 V; 0.1 M phosphate buffer containing 0.5 M KCl was the supporting electrolyte; the inset (C') and (D') shown the calibration curve for dopamine analysis for the respective modified electrode. ..... **Error! Bookmark not defined.**

Figure.5. 20. Cyclic voltammogram of (A) Ni-Fe HCFs (1:5) (B) Cu-Fe HCFs (1:1) in the absence (1) and presence of (2) 1 mM and (3) 5 mM hydrazine recorded in 0.1M $NaNO_3$ scan rate of 0.01 V s-1; (B) amperometric response of (C) Ni-Fe HCFs (1:5) and (D) Cu-Fe HCFs (1:1) modified graphite paste electrode on the addition of varying concentration of hydrazine between 0.01 μM to 5 mM; operating potential 0.3 V; 0.1 M $NaNO_3$ was the supporting electrolyte; the inset (C') and (D') shown the calibration curve for hydrazine analysis for the respective modified electrode. ..... **Error! Bookmark not defined.**

Figure.5. 21. Cyclic voltammogram of (A) Cu-Fe HCFs (1:1) and (B) Ni-Fe HCFs (1:5) in the absence (1) and presence of (2) 1 mM H_2O_2 recorded in 0.1 M phosphate buffer containing 0.5 M KCl, pH=7.0 at scan rate of 0.01 V s^{-1}; (B) amperometric response of (C) Cu-Fe HCFs (1:1) and (D) Ni-Fe HCFs (1:5) modified graphite paste electrode on the addition of varying concentrations of H_2O_2 between 0.01 μM to 5 mM; operating potential 0.0 V; 0.1 M phosphate buffer containing 0.5 M KCl was the supporting electrolyte; the inset (C') and

(D') shown the calibration curve for H_2O_2 analysis for the respective modified electrode..... **Error! Bookmark not defined.**

List of Table

Table.1.1. Electrochromic colour changes in different MHCFs. 189

Table.1.2. Curie temperature (Tc) of Prussian blue analogues. 190

Table.2.1. Characteristics of PBNPs sol as a function of H_2O_2 concentration. .....**Error! Bookmark not defined.**

Table.2. 2. Characteristics of PBNPs sol as a function of THF concentration.....**Error! Bookmark not defined.**

Table.2.3. Characteristics of PBNPs sol as a function of $K_3[Fe(CN)_6]$ concentration...**Error! Bookmark not defined.**

Table.3.1. Synthesis of Ni-Fe HCF as a function of variable composition of $K_3[Fe(CN)_6]$ and $NiSO_4$.....**Error! Bookmark not defined.**

Table.4.1. Characteristics of PBNPs as a function of PEI concentration.**Error! Bookmark not defined.**

Table.4.2. Characteristics of PBNPs as a function of $K_3[Fe(CN)_6]$ concentration.....**Error! Bookmark not defined.**

List of Scheme

Scheme.1. 1. Examples of oxidase catalyzed reactions. 212

Scheme.1. 2. Reactions involved in GOD/POD system during pathological detection of blood glucose. 213

Scheme.2.1. Scheme for THF and H_2O_2 mediated synthesis of PBNPs.**Error! Bookmark not defined.**

Scheme.2.2. Schematic presentation of colorimetric detection of H_2O_2 using PBNPs catalyzed colour reaction. ..... **Error! Bookmark not defined.**

Scheme.3.1. Schematic presentation for the synthesis of Prussian blue and Ni-Fe hexacyanoferrates..... **Error! Bookmark not defined.**

LIST OF SYMBOLS AND ABBREVIATIONS

PB	Prussian blue
PBNPs	Prussian blue nanoparticles
PW	Prussian white
PBAs	Prussian blue analogues
MHCF	Metal hexacyanoferrate
FeHCF	Iron hexacyanoferrate
NiHCF	Nickel hexacyanoferrate
Ni-Fe HCF	Nickel-Iron hexacyanoferrate
Cu-Fe HCF	Copper- Iron hexacyanoferrate
3-APTMS	3-aminopropyltrimethoxysilane
H_2O_2	Hydrogen peroxide
Hz	Hydrazine
Do	Dopamine
$HAuCl_4$	Tetrachloroaurate
THF-HP	Tetrahydrofuran-hydroperoxide
THF	Tetrahydrofuran
PEI	Polyethylenimine
GOx	Glucose oxidase
AuNPs	Gold nanoparticles
HRP	Horseradish peroxidase
CV	Cyclic voltammetry
GPE	Graphite paste electrode
CPE	Carbon paste electrode
K_m	Michaelis-Menton constant
V_{max}	Maximal reaction velocity
λ_{max}	Absorbance maxima

Preface

Selectivity in sensing process has been one of the major requisite, lack of which has restricted the practical implementation and subsequent commercialization of many chemical sensors. Chemical sensor is a device which consists of a chemically selective layer either closely related or integrated within physico-chemical transducer and has received a great attention because it provides an inexpensive, portable, and simple to operate analytical tool for identification and quantification of the specific analytes in the areas of food technology, medical engineering, environmental engineering and pollution monitoring. The use of catalytic material as chemically sensitive layer has boosted the development of chemical sensor technology and the role of nanomaterials during such development received great attention since, metal nanotubes, nanocomposites, nanorods, nanostructured polymers, nanoparticles, nanowire, different allotropes of carbons like carbon nanotubes, graphene and others lead to enhance the catalytic efficiency and selectivity during sensing process. Nanoparticles provide advantages because of their high surface to volume ratio as compared to bulk materials and has directed for specific attentions during chemical sensing as a replacement of biocatalyst during chemical sensor design.

One of the potentially explored biocatalyst is peroxidase enzyme, being used in many bioassay kits in healthcare. The susceptibility of peroxidase activity on environmental conditions directed the attention of world scientists for its replacement and the role of Prussian blue, an artificial peroxidase, has gained attention and directed for precise investigations on transition metal hexacyanoferrate. Transition metal hexacyanoferrates are the important class of extremely stable co-ordination compounds which have been used in the field like display technology, solid state batteries, hydrogen storage, cesium remediation and sensor fabrication. Amongst the transition metal hexacyanoferrates, Prussian blue is most studied, inorganic crystalline substance which have been used in various analytical applications and investigated extensively due to its electrochemical, magnetic, photophysical and electrochromic properties. However, many potential

applications, specifically as a replacement of peroxidase, are restricted due to non-processability of such crystalline material in various solvents. Accordingly the findings on the synthesis of processable Prussian blue nanoparticles have been one of requirement that constitute the theme of present research program.

The finding demonstrated that non-processability of Prussian blue and its mixed metal analogues are mainly due to uncontrolled nucleation during the synthesis of the same and directed to control the nucleation process through the participation of organic reagents. Accordingly, the synthesis of Prussian blue nanoparticles and its mixed metal hexacyanoferrate has been reported through the use of 3-aminopropyltrimethoxysinae and cyclohexanone followed by subsequent innovative development involving tetrahydrofuran hydroperoxide. These findings encouraged us to undertake the research program from the following angles: (1) Organic reagent mediated controlled synthesis of PBNPs, (2) Stabilization of PBNPs in the reaction medium itself, (3) Synthesis of PBNPs-AuNPs nanocomposite, (4) Organic reagent mediated controlled synthesis of mixed metal hexacyanoferrates of variable stoichiometric ratio of hetero transition metal ions, (5) analytical applications of Prussian blue nanoparticles and its mixed metal nanoparticles in both homogenous and heterogeneous catalysis.

The finding on thesis lines have been undertaken in the present thesis programme with specific detail given below : (1) General Introduction, (2) THF and H_2O_2 mediated synthesis of nanocrystalline PBNPs and its analytical applications, (3) THF and H_2O_2 mediated synthesis of nanocrystalline Ni-Fe hexacyanoferrates nanoparticles and its analytical applications, (4) Polyethylenimine (PEI) mediated synthesis of nanocrystalline PBNPs and its analytical applications, (5) PEI mediated synthesis of nanocrystalline mixed metal analogue nanoparticles and its analytical applications.

Chapter 1 starts with the general introduction including the results of earlier studies done on the metal hexacyanoferrates with the special attention to the Prussian blue and their application in chemical sensing.

Chapter 2 describes tetrahydrofuran (THF) and hydrogen peroxide (H_2O_2) mediated synthesis of nanocrystalline Prussian blue nanoparticles (PBNPs) and its application in hydrogen peroxide sensing. It has been found that THF in the presence of H_2O_2 allow controlled synthesis of PBNPs at 60 °C in 20 minutes under optimum ratio of reacting components. The as generated nanoparticles have been characterized through UV-Vis spectroscopy, Fourier Transformation Infrared Spectroscopy, X-Ray Diffraction analysis, Energy Dispersive Spectroscopy and Transmission Electron Microscopy. The typical application of as made nanomaterial in H_2O_2 sensing and its use as peroxidase mimetic is reported.

Chapter 3 describes THF and H_2O_2 mediated synthesis of nanocrystalline Nickel-iron hexacyanoferrates (Ni-Fe HCFs) and its application in the electrochemical oxidation study of hydrazine. It has been found that optimum concentration of $K_3[Fe(CN)_6]$, THF, H_2O_2 and $NiSO_4$ leads to the synthesis of Ni-Fe HCFs at 60 °C within 30 minutes. The as synthesized Ni-Fe HCFs have been characterized through UV-Vis spectroscopy, Fourier Transformation Infrared Spectroscopy, X-Ray Diffraction analysis, Energy Dispersive Spectroscopy, Scanning Electron Microscopy and Transmission Electron Microscopy. The effect of nickel ions on the electrochemical behaviour is also discussed. This chapter ends with the potential application of as synthesized Ni-Fe HCFs as peroxidase mimetic activity.

Chapter 4 describes polyethylenimine (PEI) mediated controlled synthesis of nanocrystalline PBNPs. It has been found that single precursors, $K_3[Fe(CN)_6]$ efficiently converts into stable, well dispersed PBNPs having excellent electrocatalytic activity. As synthesized PBNPs have been used for the synthesis of AuNPs assembled PBNPs. PBNPs and AuNPs assembled PBNPs is characterized through UV-Vis spectroscopy, X-Ray Diffraction analysis, and Transmission Electron Microscopy. These nanomaterials have been explored in both homogeneous and heterogeneous detection of H_2O_2.

Chapter-5 deals the PEI mediated synthesis of copper-iron hexacyanoferrate (Cu-Fe HCFs) and nickel-iron hexacyanoferrates (Ni-Fe HCFs)

nanoparticles. As synthesized nanocrystalline Cu- Fe hexacyanoferrates and Ni-Fe hexacyanoferrates have been characterized through XRD and TEM analysis. The effect of other transition metal ion on the electrochemical behaviour has also been investigated. These nanomaterials have been used in both homogeneous and heterogeneous catalysis for sensing of H_2O_2, hydrazine and dopamine.

The content of the thesis have been published in *Electrochimica Acta,* 190 (2016) 758–765 and *Journal Electroanalytical Chemistry*, 763 (2016) 63–70.

CHAPTER – ONE

General Introduction

1 General Introduction

Introduction of electronics in daily life has boosted the development of chemical sensors technology which is used for the measurement of phenomena and answering the obvious requirement. A chemical sensor is a combination of chemically selective layer closely related or integrated within physiochemical transducers thus dividing the sensing process in two components; (i) recognition and (ii) amplification. Selectivity in recognition event during chemical sensing has been one of the crucial which restricted the practical implementation and subsequent commercialization of many chemical sensors. Accordingly, extensive report on developing novel material has been made during last few decades and the recognition events at molecular level is being realized. However, selectivity is one of the inherent property of biologically derived material which has boosted the development of Biosensors technology, having great potentiality of commercialization. Nevertheless, the requirement of defined storage and operational conditions for biologically derived material directed the evolution of synthetic nanomaterial that can replace the biological components. Out of many biological sensing elements, peroxidase enzyme is frequently used in many bioassays, the activity of which is highly dependent on environmental conditions directing the scientific innovation in material chemistry for peroxidase replacement. Peroxidase like activity is exhibited by one of first synthetic coordination compound known as Prussian blue, a member of metal hexacyanoferrate family. However, efficiency of catalysis and processability of the same as peroxidase replacement has been serious problems for the practical viability of materials in specific concern. The present thesis work is undertaken on PB and its mixed metal hexacyanoferrate nanoparticles discussed *vide infra*.

1.1 An overview on Metal Hexacyanoferrate (MHCFs)

Prussian Blue (PB) does not occur in nature and considered to be the first synthetic coordinated compounds. PB was discovered by accidently in 1704 by a Berlin painter Heinrich Diesbach, who actually tried to create a red coloured paint [(Ware 2008)]. PB is the very first pigment which belongs to an important family

of functional inorganic materials: the transition metal hexacyanoferrates (MHCFs). PB is the simplest member of the metal hexacyanoferrate family in which both the metal centres are iron. Prussian blue and its mixed metal hexacyanoferrate have been tried to synthesize in a variety of ways by which its properties can be modulated according to the researchers need. MHCFs is famous for two quite different chemical properties: its colour, due to the mixed oxidation states of iron and its zeolytic character- a consequence of the open structure of its crystal lattice [(Ludi 1981)].

1.1.1 Crystal structure of Prussian blue

The crystal structure of PB was first explained by Keggins and Miles in 1936 on the basis of powder diffraction pattern and suggested that PB has a face-centred cubic unit cell [(Keggin and Miles 1936)]. They presumed that the interstitial metal ions such as K^+ could be accommodated in the unit cell in order to maintain the electro neutrality. Later, PB crystal structure was further explained by X-ray diffraction analysis from a single crystal obtained by slowly mixing very dilute solutions of $FeCl_2$ and $K_4[Fe(CN)_6]$ in concentrated hydrochloric acid. [(Buser *et al.* 1972; Buser *et al.* 1977)]. They revealed that the space group symmetry in Prussian blue is *Fm3m* with occupancy factor of 0.75 for Fe^{II}, C and N. Decades later, the crystal structure of PB was further explained by Ludi and co-worker using electron and neutron diffraction measurements on single crystal of PB with the space group (*Fm3m*), with a cell edge ranging between 9.9 Å and 10.9 Å [(Buser *et al.* 1972; Buser *et al.* 1977)]. The exact cell edge depends upon the specific compound and the differences reflect the metal-carbon and the metal-nitrogen bond distances. The studies done by Herren *et.al*. based on the neutron diffraction justified that PB accommodates about 14-15 water molecules in its lattice [(Herren *et al.* 1980)]. Face cantered cubic structure (space group *Fm3m*) of PB are designated in such a way that both iron centres Fe^{3+} and Fe^{2+} are bridged by the CN- groups. The Fe^{2+} ions are carbon-bound and low-spin (S=0) while the Fe^{3+} ions are nitrogen bound and high-spin (S=5/2) [(Ludi and Güdel 1973; Ohzuku *et al.* 1985)]. Prussian blue shows a long-range ferromagnetic ordering at Tc = 5.6 K in which magnetic interactions occur between Fe^{3+} ions through the 10

Å long Fe^{3+}-NC-Fe^{2+}-CN-Fe^{3+} linkages, which is the value of the cell constant [(Herren *et al.* 1980; Keggin and Miles 1936)].

There are two types of Prussian blue based on the structural variations. One is "insoluble PB" (IPB) $Fe^{III}_4[Fe(CN)_6]_3.xH_2O$ where x=14-16 and another one is "soluble" PB (SPB) $A^{I}Fe^{III}[Fe^{II}(CN)_6].yH_2O$ where y=1-5 and A is a monovalent cation such as K^+, Na^+ [(Ludi and Güdel 1973)]. Therefore, we can say that the "insoluble" form of PB differs from the "soluble" one by virtue of the excess of ferric ions which replace K^+ or Na^+ in the interstitial sites. In the literature, the term "soluble Prussian blue" was first of all used by Keggins and Miles [(Keggin and Miles 1936)]. The soluble and insoluble PB has a difference in the degree of peptization to potassium salts. Actually, both type of PB are highly insoluble (Ksp = 10^{-40}). Soluble PB undergo easily peptization with potassium salts in solution so, they are named as soluble Prussian blue. The soluble PB gives the appearance of forming a solution in water because it is easily peptized as a blue colloidal sol, which passes through a filter and does not form sediment. Therefore, the soluble form of PB stays dispersed in water. Figure.1.1 illustrates the structure the two types of Prussian blue i.e., soluble and insoluble one. [(Shokouhimehr *et al.* 2010)].

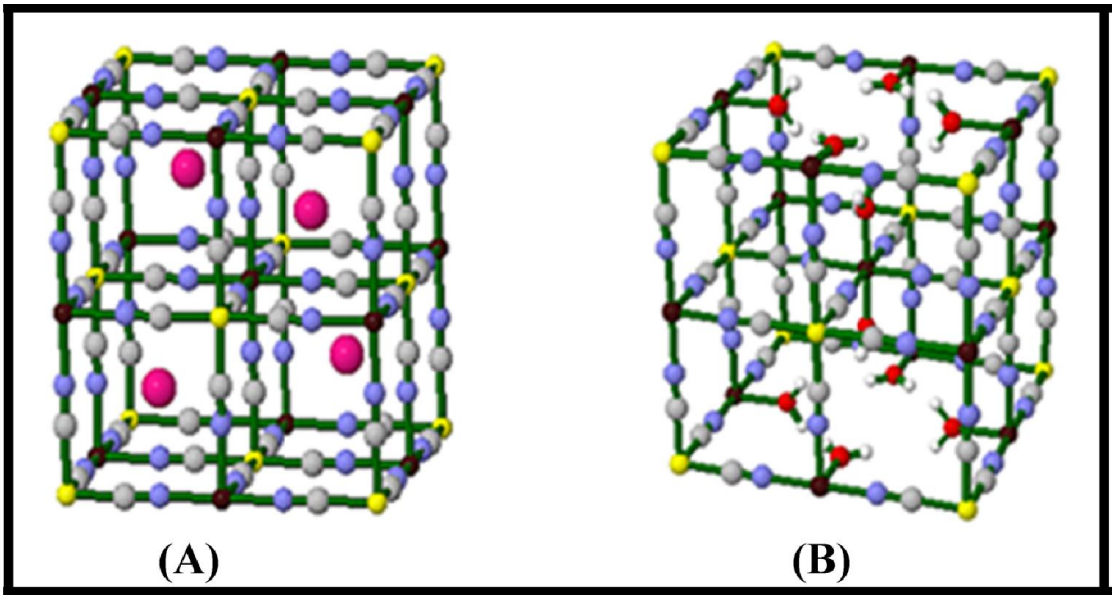

Figure.1.1. 3D structure of soluble PB (A) and insoluble PB (B), Fe(II) yellow, Fe (III) brown, K magenta, C grey, O red [(Shokouhimehr *et al.* 2010)].

In the insoluble PB, a quarter of the $[Fe^{II}(CN)_6]^{4-}$ unit is missing from the unit cell leads to an imperfect lattice, in order to maintain the charge and neutrality. This structural arrangement creates some vacant sites in the lattice that are occupied by water molecules. Beside this, the coordination sphere around the Fe (III) centre also contains the water molecules. Therefore, two types of water molecules are lies in crystal of insoluble PB: coordinative and zeolitic [(Boxhoorn *et al.* 1985)]. Due to its unique structure, PB has been commonly known as a mixed-valence coordination compound with an open zeolitic structure. The zeolitic nature of PB compounds has been extensively explored as a "chemical sponge" for absorbing low molecular weight molecules such as O_2, H_2O_2 and methane [(Boxhoorn *et al.* 1985; Imanishi *et al.* 1999; Zamora *et al.* 2010)]. This unique structural arrangement and its route to compositional variation by metal substitution as discussed *vide infra* lead to a combination of properties not readily found in other inorganic materials. Robin *et al*., was the first to emphasize that the bright blue colour of PB is due to an intervalence transition between the iron (II) and iron (III) centres [(Robin and Day 1968)].

1.1.2 Prussian blue Analogues (PBAs)

Metal hexacyanoferrate exhibits both ionic conductivity and redox properties. They constitute a class of fairly well defined zeolite-like polynuclear inorganic materials with fixed metal ion redox centres and freely diffusing cations in and out of the lattice structure during the redox processes in order to maintain electro neutrality. Among the various organometallic inorganic compounds, transition metal hexacyanoferrate have been attracted significant attention because of wide range of properties in magnetic [(Ferlay *et al.* 1995)], electrical [(Sato *et al.* 2004)], optical [(Pyrasch *et al.* 2003b)], gas storage [(Kaye and Long 2005)] and anodic material for batteries [(Nie *et al.* 2014)] and function of which can be altered by selecting a couple of metal ions composing the PB. In PB, both the iron atoms are coordinated to the -CN group while when one of the iron atom or both the iron atoms are replaced by different metal ion, a three dimensional framework of cubic symmetry is formed having octahedral coordination and the compounds are known as Prussian blue analogues (PBAs). Substitution of metal combination

leads to the synthesis of PBAs with more enhanced properties or with novel characteristics as compared to the PB. The general formula of PBAs could be represented as $A_xM[M'(CN)_6]y.zH_2O$, (where A is alkali cation which is necessary to ensure the neutrality [(Giménez-Romero *et al.* 2007)] , M and M' are same/different transition metals with same or different oxidation states in high spin and the low spin configuration respectively [(Rogez *et al.* 2001)]. In the structural study of PBAs done by Ludi and Gudel explains that the PBAs have face-centred cubic lattice in which the high spin metal and the low spin metal sites are arranged in octahedral and surrounded by –NC and –CN units, potassium as counter ions and water molecules occupy the interstitial sites [(Ludi and Güdel 1973)]. In earlier, the works done on the electrochemical behaviour and electrocatalytic activity of single transition metal hexacyanoferrates such as PB [(Karyakin and Karyakina 1999a; Karyakin *et al.* 1999; Pandey and Pandey 2013a, c)], NiHCF [(Humphrey *et al.* 1987; Wessells *et al.* 2011c)], CoHCF [(Berrettoni *et al.* 2010; Shiba *et al.* 2012; Zhao *et al.* 2014)], CuHCF [(Baioni *et al.* 2007b; Wessells *et al.* 2011b)], Manganese hexacyanoferrate [(Wang *et al.* 2013c)] and so on but later they studied hexacyanoferrate synthesized with the mixed transition metal analogues such as Ni-Co HCF, Cu-Co HCF, Fe-Ni HCF[(Pandey and Pandey 2012b)], Co-Fe HCF [(Yu *et al.* 2013)] and many more.

1.1.3 Synthesis of Prussian blue and its analogues

There are variety of methods have been published for the synthesis of MHCFs to modulate its properties. In short, there are basically two methods for the synthesis of PB, one is electrochemical [(Itaya *et al.* 1982c; Itaya *et al.* 1986; Karyakin *et al.* 1995; Karyakin and Karyakina 1999a; Karyakin *et al.* 2004)] and another one is chemical method [(Ming *et al.* 2012)]. PB is generally synthesized by mixing either Fe^{3+} ions with $[Fe(CN)_6]^{4-}$ or Fe^{2+} ions to $[Fe(CN)_6]^{3-}$ ions. One of the methods (conventional one) is based on the use of double precursor and the anther one is single precursor method. Double precursor method includes mixing of equimolar solution of $K_3[Fe(CN)_6]$ and $FeSO_4$ in the presence of a stabilizer that provides chemically and spatially confined environment for the formation of materials. Similarly, the chemical synthesis of PBAs involve the mixing of

solution of metal ions ($M^{n+)}$ to that of ferricyanide ions or electrochemically over an electrode through the application of electrochemical driving forces. Both chemical and electrochemical methods for the synthesis of PB and its analogues have merits and demerits. Synthesis of PB and its analogues through electrochemical method offers the better reproducibility and could grow directly onto the substrate which can leads to the synthesis of thin films on the electrode surface. On the negative side of this method involves that we can synthesize less amount of PB and its analogues. On the other hand, chemical synthesis of PB and its analogues could leads to large scale synthesis of PB and its analogues and also lead to synthesis of composites also. In line of this, we can divide the synthesis of PB and its analogues in two different methods. (1) Electrochemical synthesis of PB and its analogues; (2) Chemical method of synthesis of PB and its analogues.

1.1.3.1 Electrochemical synthesis of PB and its analogues

First time, in 1978, V.D.Neff reported the chemical deposition of PB over surface of platinum electrode by the involvement of $K_3[Fe(CN)_6]$ and $FeCl_3$ in the presence of potassium chloride (hereinafter KCl) and hydrochloric acid (HCl) [(Neff 1978)]. Later, Itaya *et al*. reported the synthesis of "water insoluble PB film" by electrochemical method on the different type of electrode surface [(Itaya *et al.* 1982c)]. He studied the electrochemical behaviour of PB films in solution of various supporting electrolytes like K^+, Rb^+, NH_4^+ and Cs^+. This method was used by many works to synthesize highly stable PB films on to the different electrode surface like platinum, gold, glassy carbon electrode, SnO_2, TiO_2 *etc*. (even no degradation after 10^5 cycles). There are two approaches for the electro synthesis of PB and its analogues. The most common approach is based on potentiodynamic cycling between pre set potential limits of the working electrode in a suitable supporting electrolyte containing both the metal ion (M^{n+}) and ferricyanide ions. This method has been used for the synthesis of PB and its other metal analogues like copper [(Siperko and Kuwana 1983)] and nickel [(Bocarsly and Sinha 1982; Sinha *et al.* 1984)]. In the method, metal ions are added to the ferricyanide loaded supporting electrolyte. After this, application of potentiodynamic cycling instigates the precipitation of insoluble PB and its analogues. There could be

variation in the deposition of PB films. Such as when optical transparency of films is required then conducting transparent oxide supports like tin-doped indium oxide or F-doped tin oxide glass could be used. Karyakin group has done extensive work on the electrochemical deposition of PB on the electrode surface by applying the constant potential for a fixed period in $K_3[Fe(CN)_6]$ and $FeCl_3$ solution followed by cyclic voltammetry on various electrode surface [(Karyakin 2001; Karyakin *et al.* 1995; Karyakin and Karyakina 1999a; Karyakin *et al.* 1999; Karyakin *et al.* 2004)]. Jaffari and Turner described a method for the synthesis of PB film by a simple voltammetric cycling of potassium ferricyanide solution on the surface of a graphite disk electrode [(Jaffari and Pickup 1996a; Jaffari and Turner 1997)]. Electrochemical synthesis of PB film was done by Abbaspour *et al*., with the help of potassium ferricyanide on the gold electrode and proved that it is most desirable to use a wide potential range (-0.1 to +0.9 V) with the supporting electrolyte KCl. He also suggests that the electrodeposition is highly dependent on the pH of the medium [(Abbaspour and Kamyabi 2005b)]. PB was electrochemically deposited on the carbon fibre electrode by P. Salazar *et al*., using potassium ferricyanide, ferric chloride and KCl as a supporting electrolyte which was successfully used for the detection of H_2O_2 [(Salazar *et al.* 2010)]. Yao Zhang *et al*., have electro polymerised PB film on the glassy carbon electrode/graphene oxide film and successfully utilized for the detection of H_2O_2 and glucose [(Zhang *et al.* 2011b)]. A novel photochemical method for the synthesis of PB film was described by Hu *et al*., (2005) in acidic potassium ferricyanide [(Hu *et al.* 2005)]. Here, some ferricyanide ion gets dissociated and forms free ferric ions. The crucial step in this type of synthesis is the photochemical reduction of ferricyanide ions to ferricyanide and these ferricyanide ions coordinates to the ferric ions and forms PB. In another novel method by Shou-Qing Liu (2011) explains the photoinducedly electrochemical synthesis of PB films on ITO electrode by the involvement of sodium nitroprusside. Here, a surfactant cetylmethylammonium (CTAB) cations were used to enhance the stability of PB films [(Liu *et al.* 2011)]. In another strategy for the electrodeposition of PB was done on p-Si (100) electrode with the help of potassium ferricyanide. First of all, Fe film was electrodeposited onto the silicone substrate from an acidic Fe (III) ion solution

followed by anodically stripped into the aqueous solution of potassium hexacyanoferrate (II) salt solution [(Muñoz *et al.* 2011a)]. Kumar *et al*., (2007), reported first time a one-step electrochemical deposition of gold-PB nanocomposite films [(Kumar *et al.* 2007)]. In last decade, a large number of studies come out based on the composite film of PB with other materials like gold nanoparticle-PB-graphene composite film [(Zhang *et al.* 2012b)], PB-graphite-epoxy composite [(Navarro-Laboulais *et al.* 2000)], Titanium phosphate/PB composite film [(Wang *et al.* 2007b)], PB-multiwalled carbon nanotubes composite film [(Du *et al.* 2010)] Prussian blue and multiwalled-carbon nanotubes /polyethylenimine/Au (MWNTs-PEI-Au) nanocomposites [(Zhang *et al.* 2011a)], poly(*N*-acetylaniline)–Prussian blue (PNAANI–PB) hybrid composite film [(Zhou *et al.* 2014)], graphene oxide (GO)/Prussian blue (PB) hybrid film [(Zhang *et al.* 2011b)] and many more is adding every day.

1.1.3.2 Chemical synthesis of Prussian blue and its analogues

Conventional synthesis of PB is performed by the direct mixing of solution of ferric (Fe^{3+}) and ferricyanide ions [$Fe(CN)_6^{4-}$] which leads to the synthesis of dark blue precipitate of PB. Likewise, mixing of ferrous ions (Fe^{2+}) into the solution of ferricyanide [$Fe(CN)_6^{3-}$] also gives the dark blue precipitates termed as "Turnbull's blue (TB)" which is identical to the PB due to instantaneous exchange of electrons between the ions [(Reynolds 1887)]. Later in 1968, based on the study of Mossbauer spectroscopy and X ray diffraction analysis revealed that PB and TB are same compounds regardless of the starting material [iron (III) hexacyanoferrate (II)] [(Hansen *et al.* 1969; Ito *et al.* 1968b; Maer *et al.* 1968)]. Even in case of Mossbauer spectra of PB and TB at temperature range of 1.6 k to 300 k does not show any type of valence oscillation or resonance within this complex. As for as PB synthesis is concerned, there are several points to be considered, they are: particle shape and size, reaction process, conditions of reactions, functional ability. Each of these parameters during the synthesis influences apparent solubility, colour shade, morphology (thickness, size and topography), reaction mechanism, conductivity and functional ability. There are properties which impact on the utility of the material for practical applications.

Conventional method for the synthesis of PB and its analogues is based on the direct precipitation reaction of the M^{n+} cations and the $[M'(CN)_6]^{n-}$ anions in a neutral aqueous solutions. This occurs in rapid precipitation of PB since it has very low value of solubility product (Ksp = 3.3 x 10^{-41}) [(Meeussen *et al.* 1992)] . In this type of synthesis of PB, it is difficult to control morphology and size of the reaction product. Nanotechnological development of the material in the recent years opens the area of the preparation of nanometre size PB which could leads to utilize this material for better processability, scalability and practical applications.
In the conventional method for synthesis of PB involves the two precursor ferric ions and ferricyanide ions but in last decade several studies done by researchers that are based on the single precursor like ferrocyanide or ferricyanide ions [(Hu *et al.* 2012a; Hu *et al.* 2005; Jia and Sun 2007; Ming *et al.* 2012)]. Along the synthesis of PB by single precursor, researchers also have utilized a variety of techniques and precursor to control the stability, size, shape and practical usability. Reverse microemulsion method by S Vaucher *et.al*.,(2000) [(Vaucher *et al.* 2002; Vaucher *et al.* 2000)] , PB assisted by polymers [(Hornok and Dékány 2007; Ming *et al.* 2012; Uemura and Kitagawa 2003; Yamada *et al.* 2009)], template assisted [(Johansson *et al.* 2005; Xian *et al.* 2007)], mini emulsion Periphery Polymerization (MEPP) method [(McHale *et al.* 2010)]. Wu *et al*., (2005), synthesized regular, single-crystalline PB nanocubes from a single source precursor $K_4[Fe(CN)_6]$ in acidic solution under ultrasonic conditions [(Wu *et al.* 2006)]. One of the novel methods for the synthesis of PB was done by photochemical by illuminating gold CDtrode electrode in acidic solution of $K_3[Fe(CN)_6]$ to the ultraviolet light. A blue colour film was deposited on the electrode. The key step in this synthesis is the dissociation of ferricyanide in acidic medium to form free ferric ions and HCN. Yamauchi and co-workers showed a facile method for the synthesis of highly crystalline hollow PB nanoparticles *via* controlled chemical etching method by taking PB mesocrystals as source [(Hu *et al.* 2012a)]. Ding *et al*., (2009), reported the controlled synthesis of PB crystals by the Polysaccharide (*eg.*, chitosan) hydrolysis method by using single precursor based method (acidic solution of $K_3[Fe(CN)_6]$) [(Ding *et al.* 2009)]. Reduction process was done citric acid and prepared monodispersed PB nanoparticles [(Shiba

2010)]. One of the early studies done by Uemura *et al*., (2003), synthesized water soluble, highly dispersed, PB nanoparticles protected by poly (vinylpyrollidone) (PVP) by double precursor method [(Uemura and Kitagawa 2003)] which dispersed in various organic solvents. Later, many studies were done and variation through the involvement of PVP. In the next year of this study, published by Zhonghao Li *et al*., (2004) microemulsion method was employed for the preparation of PVP protected PB nanocomposite [(Li *et al.* 2004)]. Ming Hu *et al*., (2012) synthesized the various PB analogue hollow nanocubes by chemical etching method through the protection by PVP [(Hu *et al.* 2012b)]. In another study conducted by the same group revealed that the pH value of solution, concentration of $K_3[Fe(CN)_6]$ and amount of PVP take part an active role to control the size and morphology of PB [(Ming *et al.* 2012)]. Water soluble PB and its metal analogues (FeHCF, NiHCF, CuHCF, and CoHCF) was synthesized by using (N-polyvinyl-2-pyrollidone) as a protective matrix [(Qin *et al.* 2005)]. Polyethylenimine was also used as a reducing agent and peptized material in the rapid synthesis of PB nanocubes in the refluxed solution of $FeCl_3$ and $K_3[Fe(CN)_6]$ [(Zhai *et al.* 2008)]. Jia, (2011), employed a metal complex as precursors (Fe-oxalic acid complexes) for the preparation of PB nanocrystals [(Jia 2011b)]. The fabrication of PB nanosheets by a simple hydrothermal process involving the reaction between $K_3[Fe(CN)_6]$ and glucose ($C_6H_{12}O_6$) has been reported [(Pan *et al.* 2009)]. PB nanocubes were gown on reduced graphene oxide by the involvement of double precursor and polyethylenimine [(Cao *et al.* 2010)] and on nitrobenzene fictionalized reduced graphene [(Wang *et al.* 2013b)]. In the same year, another study was performed to synthesize graphene oxide sheet- Prussian blue nanocomposite through ultrasonic wave irradiations [(Liu *et al.* 2010a)]. Qian *et al*., (20013) published a new method to prepare PB nanocubes through reduction of single-source precursor with graphene-oxide (GO) [(Qian *et al.* 2013)]. Gong *et al*., (2012) was done one step synthesis of graphene oxide-PB-chitosan [(Gong *et al.* 2012)]. Chitosan beads acts as template and stabilizing material in the synthesis of PB type nanoparticles formed by successive coordination of the transition metal ions and the hexacyanometallate precursors at the specific amino group of chitosan [(Folch *et al.* 2010)]. Alginate matrix was

also used as a template and stabilizing agents for the synthesis of water soluble Prussian blue [(Tokarev *et al.* 2012)]. Recently, ultrathin metal coordination PB nanoribbons with tunable width have been synthesized by Bao *et al*. [(Bao *et al.* 2013)]. One of the recent studies involving incorporation of PB into the ferritin complex [(Domínguez-Vera and Colacio 2003)] and capsid of cowpea chlorotic mottle virus as template [(de la Escosura *et al.* 2008; Wu *et al.* 2013)] proved that biological material could also be an effective template for entrapment of the same materials. One of the recent studies, PB nanoparticles were prepared by using cetyl pyridinium chloride as a protecting agent [(Chandra Das *et al.* 2014)].

1.1.4 Properties of Prussian blue and its analogues

1.1.4.1 Electrochemical properties of PB and its metal analogues

First of all, the electrochemical behaviour of PB in film was reported in 1978 by V.D.Neff [(Neff 1978)]. After this, the electrochemistry of PB was fully investigated by Itaya and co-workers [(Itaya *et al.* 1982c)]. The typical cyclic voltammogram of PB film consists of two redox couples with anodic peak potential values at around -0.2 V *vs*. Ag|AgCl (peak I) and 0.9 V *vs*. Ag|AgCl (peak II). Peak I is due to the oxidation-reduction response of PB to Prussian white (PW) and *vice versa*. Peak II is due to the oxidation of Prussian blue to Prussian yellow (fully oxidised form) and *vice versa* [(Ricci and Palleschi 2005)]. The response at lower positive potential (-0.2 V) results from the reduction/oxidation of a high-spin system Fe^{3+}/Fe^{2+}, while the other couple at higher positive potential (~ 0.9 V) indicates to redox reaction of low spin $[Fe(CN)_6]^{3-/4-}$. The reduction and oxidation reactions for the "soluble" and "insoluble" form of PB are different. The reduction and oxidation reactions for the "soluble" form of PB are presented as follows:

$$\underset{\text{"Soluble PB"}}{KFe^{III}[Fe^{II}(CN)_6]} + e^- + K^+ \longrightarrow \underset{\text{Prussian White}}{K_2Fe^{II}[Fe^{II}(CN)_6]} \quad (1)$$

$$\underset{\text{"Soluble PB"}}{KFe^{III}Fe^{II}(CN)_6} \longrightarrow \underset{\text{Prussian Yellow / Berlin Green}}{Fe^{III}Fe^{III}(CN)_6} + e^- + K^+ \quad (2)$$

The similar redox reaction was proposed for "insoluble" form of PB [(Ricci and Palleschi 2005)].

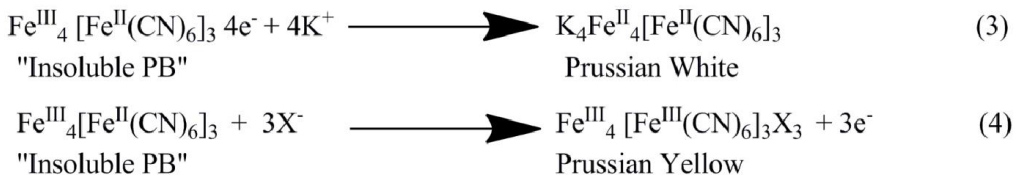

Electrochemical behaviour of PB infer that: (1) the reduction process involves the cation for both "soluble" and insoluble" forms of PB, (ii) the oxidation process involves the loss of cations for the "soluble" form and the utilization of electrolyte anions for "insoluble" form, (iii) during the oxidation and reduction process a flux of cations pass through the channels and holes of the zeolitic PB crystal structure and maintain the charge compensation. The electrochemical performances of PB films have also been investigated in the PB film. It was found that the K^+ supports the optimum electrochemical behaviour of PB [(García-Jareño *et al.* 1998)] but other cations like Rb^+, Cs^+ and NH_4^+ ions also found to maintain electrochemical reactivity of PB. On the other hand, cations like Na^+, Li^+, H^+ and other group II cations block the activity of PB after few cycles. The role of supporting electrolyte on electrochemical performances of PB film has been investigated and concluded that the cations with smaller hydrated radii freely penetrate the film, while the one with larger radii can block the process [(Karyakin 2001)]. As seen from the studies, the electrochemical behaviour can be explained on the basis of hydrated ionic radii and the channel radius of the PB lattice. PB lattice possess a channel radius of about 1.6 Å which easily accommodate K^+, Rb^+ Cs^+ and NH_4^+ whose hydrated molecules have radii less than the channel radius of PB [(Itaya *et al.* 1982a; Itaya *et al.* 1986)].

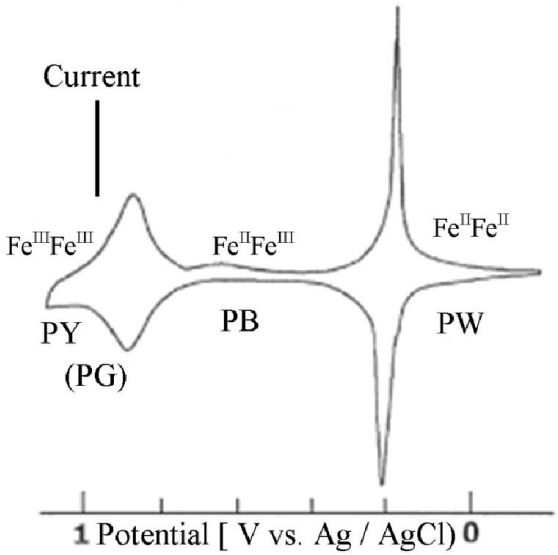

Figure.1.2. Cyclic voltammogram of a PB modified electrode showing oxidation and reduction peak [(Ricci and Palleschi 2005)]

PBAs have been synthesized by replacing one or both of the iron atoms in the PB crystal lattice. Among all the synthesized substituted PBAs, nickel hexacyanoferrates (NiHCF) shows attractive redox properties in relation to high electroactivity and distinct voltammetric response in a variety of supporting electrolytes like Li^+, Na^+, K^+ , Rb^+ and Cs^+ *etc*. This is because that the structure of both oxidised and reduced NiHCF are open enough to permit unhindered transport of alkali metal counter ions of different sizes [(Zamponi *et al.* 2003)]. The cyclic voltammogram of NiHCF shows the two redox couples at the formal potential of around 0.45 V and 0.6 V due to the redox centre of Fe^{3+}/Fe^{2+} located in two energetically different sites, i.e; the cation rich and cation deficient form of NiHCF. These two form of NiHCF can be represented as $A_2Ni[Fe(CN)_6]$ and $ANi_{1.5}[Fe(CN)_6]$ respectively. The peak at lower potential is due to the redox process of the cation deficient form of NiHCF, whereas the peak at higher potential is due to the redox process of the cation rich form of NiHCF [(Chen *et al.* 2009)].

The redox reaction of NiHCF can be represented as:

$$ANi[Fe^{III}(CN)_6] + A^+ + e^- \rightleftharpoons A_2Ni[Fe^{II}(CN)_6] \quad (5)$$

$$Ni_{1.5}[Fe^{III}(CN)_6] + A^+ + e^- \rightleftharpoons ANi_{1.5}[Fe^{II}(CN)_6] \quad (6)$$

As comparison to PB, the formal potential is shift to seen from ~ 0.9 V to ~ 0.6 V. In the case of mixed metal hexacyanoferrate (taking case of Fe^{III} and Ni^{II}), the position of the electrochemical redox peaks observed to vary gradually from ~ 0.6 V (100 % nickel) to ~ 0.9 V (100 % iron) depending upon the ratio of Fe^{III} and Ni^{II} used in the synthesis of Ni-Fe HCFs which indicate the formation of mixed crystals of Ni-Fe HCFs. The reaction of the Ni-Fe HCFs can be represented as:

$$x\,Fe^{III} + yNi^{2+} + zK^+ + [Fe(CN)_6]^{4-} \longrightarrow Fe_xNi_yK_z[Fe(CN)_6] \quad (7)$$

Here, Ni and Fe occupy the interstitial position in the crystal lattice that is why the formal potential shifts from that of pure FeHCF to that of pure NiHCF [(Reddy *et al.* 1996)]. Both iron and nickel is present in the lattice positions and affects the redox potential of Fe coordinated to carbon.

Voltammetric behaviour was explained by Siperko and Kuwana in 1983 [(Siperko and Kuwana 1983)]. In this voltammetric characterization shows a pair of redox couple with the formal potential of approximately 0.6 V. This redox potential is due to the $Cu^{II}/Fe^{II} \longrightarrow Cu^{II}/Fe^{III}$ transition and is equivalent to the last redox couple in the PB system. Similarly, the cobalt hexacyanoferrate (CoHCF) shows a pair of peaks (peak potential: Epa = 0.353 V and Epc = 0.324 V) with formal potential (Epa + Epc)/2 equal to 0.339 V ions containing electrolyte. The electrochemical behaviour of manganese hexacyanoferrate [(Jayasri and Sriman Narayanan 2007)], chromium hexacyanoferrate [(Lin and Shih 1999; Shan Lin and Feng Tseng 1998)], gallium hexacyanoferrate [(Yu *et al.* 2007a)], indium hexacyanoferrate [(Dong and Jin 1989)], palladium hexacyanoferrate [(Lezna *et al.* 2003)], zinc hexacyanoferrate [(Chu *et al.* 2007)], vanadium hexacyanoferrate [(Carpenter *et al.* 1990; Shaojun and Fengbin 1986)],

ruthenium oxide hexacyanoferrate [(Paixão and Bertotti 2008b)] and silver hexacyanoferrates have also been reported in many works. The electrochemical behaviour of rare earth based hexacyanoferrates were also investigated by many research groups like Cerium hexacyanoferrate (CeHCF) [(Feng *et al.* 2009)], lanthanum hexacyanoferrate (LaHCF) [(Liu and Chen 2002)], dysprosium hexacyanoferrate (DyHCF), samarium hexacyanoferrates (SmHCF) [(Wu and Cai 2005)], neodymium hexacyanoferrate (NdHCF), terbium hexacyanoferrates (TbHCF) and erbium hexacyanoferrates (ErHCF) by Sheng *et al*., 2007 [(Sheng *et al.* 2007a)]. In another work, Europium hexacyanoferrate (EuHCF) film was electrodeposited on the graphite electrode with a well defined peak at 0.7 V and confirmed by XPS that the valences of Fe in the film were changed during the electrochemical reaction. Electrochemical behaviour of rare earth hexacyanoferrates with composite was also done in order to modulate the material for their own need. Fang *et al*, (2007) studied the electrochemical behaviour of cerium hexacyanoferrate (CeHCF) with multiwalled carbon nanotubes [(Fang *et al.* 2007)]. Electrochemical behaviour of Samarium hexacyanoferrate (SmHCF) and lutetium hexacyanoferrate (LuHCF) with graphene oxide nanocomposite material was also investigated [(Devadas *et al.* 2014a; Devadas *et al.* 2014b)] and yttrium hexacyanoferrate with carbon nanotubes was also studied by Lingbo Qu *et al*; 2010 [(Qu *et al.* 2011)].

1.1.4.2 Electrochromic properties of PB and its metal analogues

An electrochromic material have the property of a colour changes in a persistent but in reversible manner in response to either an electron transfer process (redox process) or by a sufficient electrochemical potential. The electrochromic materials can be classified as reduction and oxidation colouring material depending on the colouring mechanism. Generally the colour change is between a transparent (bleached) state and a coloured state or between two different coloured state. In some cases, more than two electrochemical redox states are available, the material exhibit several colours and termed as polyelectrochromic material. There are several material showing electrochromism like transition metal oxide (inorganic electrochromic material) *e.g*., tungsten [(Di

Paola *et al.* 1978; Hurditch 1975)], manganese [(Burke and Murphy 1980b)], cobalt [(Burke *et al.* 1982)], iridium [(Burke and Whelan 1984)], rhodium [(Burke and O'Sullivan 1978)], ruthenium [(Burke and Murphy 1980a)], Phthalocyanines, viologens and Buckminsterfullerene, polypyrrole, polyaniline, polythiophene and PB. Electrochemical and Electrochromic behaviour of PB was not studied until lack of knowledge of synthesis of thin film of PB. So, the first report concerning the electrochemical and electrochromism behaviour was done by Neff, 1978 [(Neff 1978)]. However, the PB based electrochromic devices that utilizes sole material PB as electrochromic was done by Itaya, 1982 [(Itaya *et al.* 1982c)]. PB can be electrochemically reduced and change into colourless form 'Prussian white" (PW, Everitt's salt) and oxidised and change into pale green form "Prussian green" (PG, Berlin green). Earlier studies revealed that an electrodeposited PB exhibits electrochromism between blue and colourless state with a fast response (≤ 100 ms) and a highly stability for $5x10^6$ cycles [(Itaya *et al.* 1982d)]. This behaviour makes PB as an ideal candidate for the electrochromic devices (ECD). The colour change of PB, a typical oxidation colouring material is as follows:

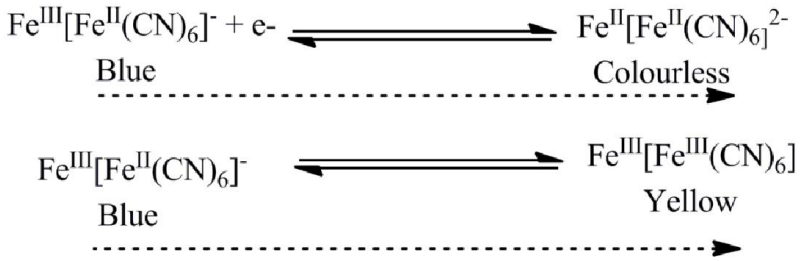

PB can readily be oxidised to colourless substance (PW) so, the thin film of PB can be made transparent by the reduction reaction and the transparent films darkened by oxidation. Electrochromic contrast can be improved through the involvement of complementary active component with the PB in the film preparation. Such combination exhibits unusual property and unique design possibilities. PB has been used to construct composite material for electrochromic devices like WO_3 [(Ashrit *et al.* 1993; Ho *et al.* 1994)], TiO_2 [(Campus *et al.* 1999)], V_2O_5 [(Ashrit *et al.* 1993)],$Ta_2O_5.nH_2O$ [(Sone *et al.* 1996)] or organic conducting polymers like polyaniline [(DeLongchamp and Hammond 2004b;

Kulesza *et al.* 2001)], Poly(pyrolle) [(Keiichi *et al.* 1983)], benzylviologen and Poly(3-methylthiophene) [(Leventis and Chung 1992b)] and Poly(vinylpyrollidone) [(Leventis and Chung 1992a)] other materials like carbon nanotubes [(Nossol and Zarbin 2013)], heptyl viologen solution [(Lin *et al.* 2011a)] and many more study have been done to improves the electrochromic property of PB.

PB based material has its unique structure and can be easily modulate the compositional variation by other metal substitution leads to a wide spectrum of PBAs making a colour change which can easily be exploited in the electrochromic devices. For example, reddish brown-to-yellow, reddish brown-to-green,, yellow-to-colourless, green-to-blue-to-colourless and purple-to-colourless electrochromism are shown by CuHCF [(Baioni *et al.* 2007b)], CoHCF [(Gao *et al.* 1991)], NiHCF [(Kulesza *et al.* 2001)], FeHCF and Ruthenium hexacyanoferrate (RuHCF) respectively [(de Tacconi *et al.* 2003)]. The reason for electrochromism in PB and its mix metal analogues is due to the valence change of one of the component metal centres in the crystal causes a simultaneous change in the charge transfer oscillation energy and which could leads to the change in the colour of the crystal. PBAs CoHCF is a peculiar electrochromic material, its colour is not only dependent on the oxidation state of the metal centre but also on the nature of the counter cations. The oxidised CoHCF film shows purple brown colour in potassium or cesium (hydrated) ions and sodium electrolyte while during reduction the film turns olive-brown in 1 M KCl and becomes green in 1 M NaCl or lithium (hydrated) ions [(Kulesza *et al.* 1995b)]. CoHCF is not only electrochromic but it is thermochromic also. In the case of CuHCF, it is shown that during voltammetric experiments that only the $Cu^{II}Fe^{II} \longrightarrow Cu^{II}Fe^{III}$ redox process takes place, indicate that Cu^{II} ions does not change the oxidation state. DeLongchamp and Hammond (2004) studied the electrochemic behaviour of PB / linear poly (ethyleneimine) nanocomposite film and proved that an optimum thickness with maximum contrast was expected to lie beyond 60 layer pairs [(DeLongchamp and Hammond 2004a)]. A summary of electrochromism of various MHCFs is given in following Table.1.1:

Table.1.1. Electrochromic colour changes in different MHCFs.

MHCFs	Colour	
	Reduced state	**Oxidised state**
FeHCF	Colourless	Yellow or light green
CuHCF	Reddish brown	Yellow
NiHCF	Light grey	Yellow
PdHCF	Green	Orange
InHCF	White	Yellow
VHCF	Yellow	Blue-green
CoHCF*	Green	Yellow

*colour depends on various factors like presence of ions in the electrolyte etc.

An investigation shows the electrochromic thin film of PBNPs dispersible into various solvents by mutual coordination bonding and wet process [(Ishizaki *et al.* 2009; Shigeo *et al.* 2007)]. Electrochemical and electrochromic properties of PB was enhanced by the use of surface active agents like cetyltrimethyl ammonium bromide (CTAB) [(Vittal *et al.* 1999)].

1.1.4.3 Magnetic properties of PB and its metal analogues

PB and its mixed metal analogues is the member of coordination polymers and kind of molecular magnets. Researchers have given a great attention for molecular based magnets due to several reasons for example, they can be easily synthesizes at room temperature with a well defined $[M(CN)_6]^{n-}$ building blocks, the metal spin carriers are linked covalently into 3D-cubic network, a wide range of different spin states and oxidation states can be achieved by simply substituting the other metal ions. Cyanide bridge ligands of PB and analogues provide a way for the exchange of magnetic information between paramagnetic centres. The first report on the magnetic susceptibility of PB was performed by Davidson and Welo in 1928 [(Davidson and Welo 1928)]. Here, no information about the magnetic ordering could get because of the study was restricted to temperature between 200

- 300 K. After 40 years of this, based on the Mossbauer study, Ito *et al.*, (1968) reported the ferromagnetic type behaviour of PB low temperature with the Tc = 5.5 ± 0.5 K [(Ito *et al.* 1968a)]. Bozorth *et al*., (1956) reported a series of PB analogues based magnet prepared by adding Mn^{II}, Fe^{II}, Co^{II}, and Cu^{II} to $[Fe^{III}(CN)_6]^{3-}$, $[Mn^{III}(CN)_6]^{3-}$ and $[Cr^{III}(CN)]^{3-}$ with the curie temperature ranging from 3 K to 50 K [(Bozorth *et al.* 1956)]. PB itself has shown the ferromagnetic properties at low Curie temperature. The low Curie temperature is due to the long range ferromagnetic ordering. Due to the diamagnetism of low spin d^6Fe^{II} centres (which occupy the strong ligand-field sites) through-bond distance between paramagnetic high-spin (d^5Fe^{III}) centres has been over 10 Å in length, leads to weak exchange coupling. In the case of PB analogues, all the metal centres are paramagnetic, so the through-bond distance between nearest spin centres is reduced from 10 Å to about 5 Å, resulting to the stronger exchange coupling. Thus, Curie temperature (Tc) of PB analogues has higher value than the PB alone and this has been confirmed by many authors. Following Table.1.2. showing Curie temperature of some PBAs.

Table.1.2. Curie temperature (Tc) of Prussian blue analogues.

Compound	Ordering Nature	Tc / K	Reference
$Ni^{II}[Fe^{III}(CN)_6]_{2/3}.nH_2O$	Ferro	23	[(Juszczyk *et al.* 1994)]
$Cu^{II}[Fe^{III}(CN)_6]_{2/3}.nH_2O$	Ferro	20	[(Hatlevik *et al.* 1999)]
$Co^{II}[Fe^{III}(CN)_6]_{2/3}.nH_2O$	Ferri	14	[(Hatlevik *et al.* 1999)]
$Mn^{II}[Fe^{III}(CN)_6]_{2/3}.nH_2O$	Ferri	9	[(Hatlevik *et al.* 1999)]
$Fe^{II}[Fe^{III}(CN)_6]_{2/3}.nH_2O$	Ferro	5.6	[(Marvaud *et al.* 2003)]

The magnetic properties of PB and its analogues are governed by the electronic structure of the transition metal ions bridged to the cyanide linkage. As seen from the magnetic study, mixed valency vanadium provide the highest Curie temperature within the PBA family reported earlier [(Verdaguer *et al.* 1999a; Verdaguer *et al.* 1999b)]. The highest Curie temperature reported so far is Tc = 376 K for the compound $[KV^{II}[Cr^{III}(CN)_6]_z]$ by [(Garde *et al.* 2002)], another one is $[V^{II}[Cr^{III}(CN)_6]_{8/3}.nH_2O$ Tc = 315 K by [(Ferlay *et al.* 1999)] and $[V^{IV}O[Cr^{III}(CN)_6]_{8/3]}.nH_2O$ Tc = 115 K. Magnetic measurement performed by Pingheng Zhou *et al*., showed that the Curie temperature of PB nanowire decreases as the average number of magnetic interaction neighbours is decreased [(Zhou *et al.* 2002)]. Uemura group, synthesized the Poly(vinylpyrollidone) protected PBNPs and report the size-dependent control of the magnetic property of the coordination polymers [(Uemura and Kitagawa 2003)]. They showed the increase in Tc while increasing the nanoparticles size with the maximum Tc for bulk PBNPs (5.5 K). After two years of this, Sun *et al*., showed the shape dependent magnetic properties in PBAs material $SmFe(CN)_6.4H_2O$ [(Sun *et al.* 2005)]. They proved that the shape of the low-dimensional nanoscale material is a dominating factor for its coercivity due to the effect of shape anisotropy. In another study, PB was synthesized on the alginate beads and showed the superparamagnetic, spin-glass or paramagnetic behaviour depending upon the nature of metal ions used. In case of $Ni^{2+}/[Fe(CN)_6]^{3-}$/alginate and $Cu^{2+}/[Fe(CN)_6]^{3-}$/alginate exhibit the spin-glass behaviour while in case of $Mn^{2+}/[Fe(CN)_6]^{3-}$/alginate nanoparticles shows superparamagnetic behaviour [(Tokarev *et al.* 2012)].

1.1.4.4 Charging and discharging characteristics of PB and its metal analogues

It is well known that PB and its metal analogues intercalate alkali metal cations reversible during the redox electrochemical transformation. In spite of this the intercalation-deintercalation cycle does not lead to any changes in the crystal lattice. The other interesting characteristic of PB lies in terms of highly reversible redox property to the order of 10^5 cycles and 10^7 cycles when electrochemically deposited on ITO and SnO electrode respectively. These two major properties i.e,

reversibility and stability make PB for the suitable candidate for the battery application. In 1978, V.D.Neff reported that PB could be used as cathode and anode material for secondary cell [(Neff 1978)]. Later, some studies pop up about the thermodynamic and kinetic characteristics of the electrochemical oxidation and reduction of PB thin film [(Ellis *et al.* 1981; Itaya *et al.* 1982a)]. Three years of this study, PB based secondary battery have been fabricated based on the pair of PB coated electrode [(Kaneko 1986; Neff 1985)] or PB was chemically deposited on the Nafion film on both the surfaces [(Honda *et al.* 1986)]. All these studies were based on electrochemical but not spectrophotometrical. Both electrochemical and spectrophotochemical studies of PB based secondary battery was done by Masao Kaneko in 1988 and proved that the electrochemical redox reactions must be slow in thicker film PB in comparison to thinner film of PB [(Kaneko and Okada 1988)]. Another approach for secondary cell with PB and CuHCF thin layers on platinum were used as anode and cathode respectively [(Grabner and Kalwellis-Mohn 1987)]. In 1999, F. Scholz group have used PB as both cathode and anode material for the construction of PB secondary cell and studied the charge-discharge characteristics of solid state secondary cell [(Jayalakshmi and Scholz 2000a)]. To overcome the problems generated in this he studied Iron hexacyanoferrate (FeHCFs)acted as active solid material for cathode and zinc hexacyanoferrate (ZnHCF) and copper hexacyanoferrate (CuHCF) as anodic material and studied the charge-discharge characteristics. He proved that the recycling efficiency of ZnHCF was better than the CuHCF [(Jayalakshmi and Scholz 2000b)]. Ali Eftekhari fabricated solid-state secondary cell by employing (i) Chromium hexacyanochromate (CrHCC) as anode and chromium hexacyanoferrate (CrHCF) as a cathode material, (ii) potassium anode and PB as cathode (iii) Chromium hexacyanochromate (CrHCC) as anode and PB as cathode material. The resulting secondary cell gave the superior performance over other in terms of relatively high voltage about 1.5 V and excellent cyclability for more than 500 reversible cycles [(Eftekhari 2003, 2004a, b)]. Recently, high quality PB crystals were synthesized with low crystal water content and a small number of $[Fe(CN)_6]^{3-}$ vacancies and proved that water content and vacancies affect significantly on the electrochemical performances as cathode materials for Na-ion

batteries [(You *et al.* 2014)]. Charge transfer kinetics and cyclic stability are the two key variables that is required further optimization for PB and other MHCF compounds in order to effectively compete with other available alternatives. Recently, Cui and co-workers have reported stable Na^+ cyclability into potassium copper hexacyanoferrate in an aqueous electrolyte but here the drawback is an electrolyte limits the stable voltage of a rechargeable battery to 1.5 V [(Wessells *et al.* 2011a; Wessells *et al.* 2011c)]. Manganese hexacyanomanganate, sodium zinc hexacyanoferrate and sodium manganese hexacyanoferrate were used as a effective material for cathode in sodium ion batteries [(Lee *et al.* 2014; Lee *et al.* 2012; Wang *et al.* 2013a)].

1.1.4.5 Photophysical properties of PB and its metal analogues

Photophysical properties pertain to the physical effects of light. In line of this, photo response of PB and its analogues based material is getting so much attention to optical sensor and solar energy conversion [(Koncki *et al.* 2001a)]. PB has high molar mass and polynuclear mixed-valent iron cyanide complex, and a p-type semiconducting character that is why PB and its analogue has been an attractive subject of study especially in photo electrochemical reactions [(Muñoz *et al.* 2011b)]. Certain material after deposition on the semiconductor surface, acts as an agent which facilitate transfer of either electrons or holes into the species in solution for example: Platinum or other noble metals acts as electron transfer agents when coated on semiconductor. In contrast to that, ruthenium dioxide or manganese dioxide acts as hole transfer agents. Like this PB and its mixed metal analogues acts as hole transfer agents in photoelectrochemical process [(Christensen *et al.* 1985; Koncki 2002)]. Paul *et al*, (1984) proved by pulse radiolysis experiment that PB catalyzes the oxidation of water to O_2 with $bipy_3Ru^{3+}$ as oxidant. This oxidation was done only in the presence of a sacrificial electron acceptor [(Christensen *et al.* 1985)]. Kaneko *et al*., (1985) reported that photo-response character of PB coated over basal plane pyrolytic graphite [(Kaneko *et al.* 1985)]. Kaneko *et al*., have reported that irradiation of water containing $Ru(bpy)_3^{2+}$ and PB gave simultaneous evolution of hydrogen and oxygen by water photolysis and concluded that during photolysis the electron

transfer from the excited state of the Ru complex to PB [(Kaneko *et al.* 1986)]. Thus, electrodeposited film must provide a photoresponsive electrode surface. The photocurrent responses of PB modified glassy carbon electrode in KCl solution in the presence and absence of the I^-/I_2 redox system was examined by Upadhyay *et al*., (1991) [(Upadhyay *et al.* 1991)]. Zhao *et al.,* have studied the static quenching of photoluminescence from copolymer pendant complexes by colloidal PB and analyzed in terms of step wise complex formation mechanism between pendant $Ru(bpy)_3^{2+}$ and negatively charged PB [(Zhao *et al.* 1998)]. Deposition of PB on cadmium sulphide electrode have increased the photocurrent quantum efficiency of a polycrystalline cadmium sulphide anode in KI + I_2 solution which proved that PB film catch the holes generated in cadmium sulphide and effectively transfers to the redox species in solution [(Tennakone *et al.* 1994)]. In another study, PB was deposited on p-Si (100) silicon wafer and characterize on that by means of cyclic voltammetry under illuminations condition which indicate the presence of redox processes related to high and low-spin iron centres which present in a quasi-reversible behaviour. The photoelectrochemical properties of Langmuir-Blogett (LB) films containing PB and a surfactant were analyzed and photoactivity was found to be proportional to the number of deposited layers [(Ravaine *et al.* 1998)]. Photoelectrochemical properties of TiO_2-PB nanocomposite was also studied and realized the switching of the photocurrent direction under influence of electrode potential [(Szaciłowski *et al.* 2006)].

1.1.5 Properties of Mixed metal hexacyanoferrates (MHCFs)

Study of MHCFs attracted to researchers because of their properties which can be modulated by varying its composition. The zeolitic structure of PB allows the electron and ion diffusion because of which the charge balance is maintained in the PB structure. Not only this but intercalation of transition metal ions are also lead to occupy the interstitial position as well as substitute the regular sited nitrogen-coordinated metal ions, i.e., the high-spin iron of PB. As far as structure is concerned, PB analogues contains cubic structure where the carbon atom in the cyanide groups coordinated to iron ion and the nitrogen atom coordinates to metal ions at the cube edge [(de Tacconi *et al.* 2003)]. In PB analogues, nitrogen

coordinated metal ions varies to another bivalent ions and forms not only simple MHCFs but also complex hybrid MHCFs. Therefore, when two different transition metal ions are coordinated to the nitrogen atoms then mixed MHCFs are formed. In MHCFs both the coordinated metal atoms gives the effect that leads to the variable catalytic efficiency relevant to transition metal ions related to parent PB material.

MHCFs have great attention due to various applications such as in electrocatalysis, solid-state batteries, ion-exchange selectivity, electrochromism, photophysical properties and magnetic properties. Not only, most studied metal hexacyanoferrates were transition metal atoms, such as copper (II), cobalt (II), nickel (II), tin (II), silver and ferric (II) but also rare earth metals like lanthanum [(Liu and Chen 2002)], cerium [(Fang *et al.* 2007; Feng *et al.* 2009; Yang *et al.* 2011)], terbium [(Sheng *et al.* 2007b)], europium [(Liu *et al.* 2010b)] and yttrium [(Qu *et al.* 2011; Roka *et al.* 2006)] were also studied.

As far as synthesis of MHCFs is concerned, this can be synthesized in film as well as bulk powders. First report on the Iron-ruthenium complex was done by Itaya group [(Itaya *et al.* 1982b)]. First report on mixed Fe-Ni hexacyanoferrates (Fe-Ni HCFs) was done by Bharathi *et.al*., (1992) on glassy carbon electrode and realized the multi-electron transfer centre [(Bharathi *et al.* 1992)] . They also postulated that replacement of the outer sphere Fe^{2+}, partially or completely, by other transition metal ions are structurally compatible in a host-guest assembly manner. In 1996, Reddy *et.al*., synthesized the crystalline mixed metal Fe-Ni HCFs by co-precipitation of Fe^{3+} - Ni^{2+} - HCFs and inferred that mixed crystals of Fe-Ni HCFs are formed by replacing the nitrogen coordinated iron by nickel in the crystal lattice as the percentage of nickel increases. Thin transparent film of Ni-Fe HCFs was synthesized and electrochemically studied by Yamada *et.al*., over ITO electrode with a transparent oxidation and reduction states [(Yamada *et al.* 1997)]. Mixed iron-cadmium hexacyanoferrates and iron-copper hexacyanoferrates was studied through solid-state electrochemical, X-ray diffraction, spectroscopic analysis and revealed the following findings: (i) the comparable ionic radii of Fe_{hs}^{3+} (78.5 pm) and Cu^{2+} (87 pm) together with the possibility of charge compensation by K^{+} ions, reflect the formation of mixed crystals of substituted

hexacyanoferrates; (ii) the difference between the ionic radii of Fe_{hs}^{3+} and Cd^{2+} (109 pm) is too large to allow the formation of simple substituted mixed MHCFs but the zeolitic structure of same allows the system much more degrees of freedom, resulting into a stable lattice [(Schwudke *et al.* 2000; Zakharchuk *et al.* 1999)]. Scholz group have studied various type of mixed metal hexacyanoferrate by an electrochemical driven insertion- substitution mechanism such as nickel-iron, cadmium-iron, cadmium-silver etc. Kulesza *et al*., (2000) have synthesized and characterized electrode modified with mixed hexacyanoferrates of nickel – cobalt and nickel – palladium and provided the unique voltammetric and electrochromic behaviour in comparison to the single mixed metal analogues [(Kulesza *et al.* 2000; Kulesza *et al.* 1999; Kulesza *et al.* 1995a)]. Both the system, hybrid metal hexacyanoferrate showed the different voltammetric and electrochromic characteristics in comparison to single component MHCFs. Cobalt-iron hexacyanoferrate have been studied and proved that cobalt atom are found in both high spin (Co^{II}) and low spin (Co^{III}) while iron is only found in low spin state [(Martínez-García *et al.* 2007)]. Copper-cobalt HCFs was electrochemically deposited on modified carbon paste electrode and explored the possibility for the oxidation of L-cysteine [(Abbaspour and Ghaffarinejad 2008)]. Composite thin film of mixed nickel (II) and thallium (I) hexacyanoferrates (III), (II) have synthesized through electrodeposition on the electrode surface and proposed that thallium ions are expected to locate at the interstitial position of NiHCF [(Kukulka-Walkiewicz *et al.* 2001)]. Hybrid nickel-cobalt hexacyanoferrate particles have been reported and proved that Ni-Co HCFs is a substitution type hybrid hexacyanoferrate rather than simple mixture system [(Shi *et al.* 2005)]. A study performed by Xingpin Cui (2002) based on the electrodeposition of copper – cobalt hybrid hexacyanoferrate showed the activity over wide range of pH and the relative concentration ratio of copper to cobalt have great impact on the electrochemistry and lattice constant of Cu-Co HCF [(Cui *et al.* 2002)]. Cu-Co HCF showed different electrochromic and electrochemical behaviour of single metal hexacyanoferrates. Lorella Guadagnini and co-workers performed the studies of mixed hexacyanoferrates of Cu and Pd (Cu-Pd HCFs) which was potentiodynamically grown on glassy carbon surfaces [(Guadagnini *et*

al. 2010)]. Recent studies on the preparation of mixed MHCFs film using a combination of Ni-Fe [(Kumar *et al.* 2011)], Co-Fe [(Yu *et al.* 2013)] and Ba-Ni , Co-Ni , Co-Pb, Co-Cu, Cu-Ni, Cu-Pb, Mn-Ni, Ni-Pb have also been reported [(Ghaffarinejad *et al.* 2012)]. In addition to that, Manabu Ishizaki and group demonstrated the preparation of highly dispersible mixed metal PBNPs ($Fex Niy[Fe(CN)_6]_2.zH_2O$ [(Ishizaki *et al.* 2010)]. In the field of rubidium-manganese hexacyanoferrate a significant studies have been done by Hioko Tokoro group in relation of magnetic field [(Tokoro *et al.* 2007; Tokoro *et al.* 2008; Tokoro *et al.* 2004)].

1.2 Prussian blue and its mixed metal analogue in analytical applications

The findings reviewed in preceding sections revealed that PB has been an attractive candidate for its use in the field of electrochromism, photoimaging, ion sensing, photoelectrochemical and photocatalytic devices, photomagnetic devices, batteries and electrocatalysis.

Electrochemical applications of PB and its mix metal analogues are one of the most important applications in the analytical usage of this material. Electrochemical applications of PB `has been evaluated, as chemically modified electrode (CMEs), prepared by modifying a chemically unproductive surface or bulk into chemically predictive one by the addition of a selective monomolecular, multimolecular/polymeric chemical film or composite materials attached on the electrode surface. Metal hexacyanoferrates have been extensively used in the construction of chemically modified electrode for the electrochemical detection of various analytes. Due to high chemical, electrochemical stability and simple preparation, these metal hexacyanoferrates have gain attention in practical applications. Metal hexacyanoferrate based chemically modified electrodes can be fabricated [(Pournaghi-Azar and Dastangoo 2002)] by one of the following ways: (A) Inert electrode surface immersed in a solution containing ferricyanide and transition metal ions and then applying potential to the electrode (Electrochemical deposition of metal hexacyanoferrates over inert electrode surface); (B) Immersing the transition metal electrode surface in a hexacyanoferrate ions solutions and the

electrochemical anodizing of the electrode (Electrodeposition of metal hexacyanoferrate over transition metal electrode surface); (C) Electrodeposition of the transition metal on the suitable matrix and the electrochemical anodizing of resulting surface in the presence of hexacyanoferrate ions (Electrodeposition of metal hexacyanoferrate over suitable matrix); (D) Electrodeposition of the transition metal on the matrix and then chemical derivatization of the resulting electrode in the presence of hexacyanoferrate ions; (E) Deposition of the transition metal on the matrix by electroless and then chemical derivatization of the as prepared surface in the presence of hexacyanoferrate ions; (F) Self-assembly of a monolayer of an organofulfur compounds (SAM) on a gold electrode, with certain second chemical functionality, this could be derived with a metal-hexacyanoferrate; (G) Attachment of insoluble metal hexacyanoferrate mechanically as micro- particles to the surface of appropriate electrode, e.g. paraffin impregnated graphite electrode; (H) Immobilization of metal-hexacyanoferrate in the polymer matrix and the attaching it to the electrode surface.

Most commonly used electrode surface in the construction of chemically modified electrodes are platinum, gold, aluminium, Indium tin oxide electrode (ITO electrode), F-doped tin oxide electrode (FTO electrode) SnO_2 electrode, TiO_2 electrode, clay modified electrode, glassy carbon electrode, carbon paste electrode and screen printed electrode etc.

1.2.1 Electrochemical applications of Prussian blue and its mixed metal analogues

PB and its mixed metal analogues have been an outstanding material and extensively explored for the development of electrochemical sensors. Electrochemical applications of PB can be categorised in following ways and will be discussed under each category step by step.

1.2.1.1 Electrochemical sensor for oxidizable species

PB and its mixed metal analogues have been used for the detection of oxidizable organic and inorganic compounds. Most commonly compounds used

for the oxidation study by PB and its mixed metal analogues are ascorbic acid, cysteine, dopamine, hydrazine, catecholamine, Nicotinamide adenine dinucleotide (NADH), cyctochrome C, sulphite, persulfate anion, sulfhydryl, sulphur dioxide, thiosulfate etc. In addition to the utilization of PB and its mixed metal analogues, the composite and nanocomposite material was also used to the detection of these oxidizable compounds. The oxidative mechanism of ascorbic acid was published in 1986 by Hu *et al*., on glassy carbon electrode [(Hu and Kuwana 1986)] but the first report on the utilization of PB in the electrochemical oxidation of ascorbic acid was done in 1987 by Fengbin Li *et.al*., on the galvanostatically deposited thin film over glassy carbon electrode [(Li and Dong 1987)]. This has opened the possibility to utilize the PB in the study of oxidizable species. Later, the same group have studied the electrochemical oxidation of ascorbic acid by PB film over microdisk electrode [(Dong and Che 1991)]. Later on, the utilization of nickel hexacyanoferrate, copper hexacyanoferrate and cobalt hexacyanoferrate was also studied in an effective way [(Cai *et al.* 2000; Shankaran and Narayanan 1999; WANG *et al.* 1992)]. PB based optical sensor, flow injection analysis system have been used for the determination of ascorbic acid which is based on the principle of conversion of Prussian blue to Prussian white in the presence of reductant analytes [(Lenarczuk *et al.* 2001a)]. Detection of ascorbic acid on the electrochemically deposited PB on glassy carbon electrode by flow injection analysis was also done by Suely S.L. Castro *et al*., (2001) [(Castro *et al.* 2001)]. Sheng *et al.,* (2007), fabricated sol-gel derived terbium hexacyanoferrate modified carbon ceramic electrode (CCE) and the electrochemical sensing of ascorbic acid (AA) was examined based on amperometric measurement [(Sheng *et al.* 2007b)]. Hosseinzadeh *et al*., (2009), analyzed the effect of cetyltrimethyl ammonium bromide (CTAB) for the determination of dopamine (DA) and ascorbic acid (AA) based on tin hexacyanoferrate modified carbon paste electrode and the electrochemical observation proved that cationic surfactant, CTAB enables the separation of the oxidation peak potential of AA and DA. Recently, a self-powered sensor for AA has been developed by Zloczewska *et al*., (2013) based on PB displays as an indicator [(Zloczewska *et al.* 2014)]. In one of the earliest work, Welymg Hou (1992) have successfully studied the electrocatalytic oxidation of

hydrazine over PB modified glassy carbon electrode in flow injection analysis system [(Hou and Wang 1992)]. Mechanistic aspect of electrochemical oxidation of hydrazine over PB modified glassy carbon electrode was studied Ursula Scharf in 1996 and proved that the PB based electro-oxidation of hydrazine is first order with respect to the concentration of the catalyst Fe^{III} sites and to the concentration of hydrazine [(Scharf and Grabner 1996)]. After successfully studied the possibility for exploration of PB in the detection of hydrazine, its metal analogues have been used for the detection of same. NiHCF, manganese hexacyanoferrate and zirconium hexacyanoferrate have been successfully used for the detection of hydrazine on the electrochemical deposition of PB on carbon ceramic electrode [(Jayasri and Narayanan 2007; Salimi and Abdi 2004)]. A comparative study for the electro-oxidation of hydrazine over different metal hexacyanoferrate was done and reported that the catalytic efficiency on manganese, zinc and indium is the highest [(Narayanan and Scholz 1999)]. Copper-cobalt mixed metal hexacyanoferrate film was electrochemically deposited on the surface of graphite paste electrode and successfully used for the detection of hydrazine [(Abbaspour and Kamyabi 2005a)]. Functionalized graphene with electrodeposited PB/single walled carbon nanotubes, PB/multiwalled carbon nanotubes and chromium hexacyanoferrate/multiwalled carbon nanotubes in different studies was also used for the detection of hydrazine and hydroxylamine [(Fang *et al.* 2009; Gholivand and Azadbakht 2011; Jiang *et al.* 2011; Wang *et al.* 2010; Zhang *et al.* 2010a)]. Metal hexacyanoferrate and its mixeded metal hexacyanoferrate and also with other material formed nanocomposite have been used for the electrochemical detection of L-cysteine by several groups [(Abbaspour and Ghaffarinejad 2008; Majidi *et al.* 2010; Qu *et al.* 2011; Sattarahmady and Heli 2011)]. A general kinetic model for the calculation of Cys sensing current was developed by Chen *et al*. (2006) based on the Indium hexacyanoferrate, a metal analogue of PB. The kinetic model takes both effects of Cys diffusion and electrocatalytic reaction into consideration and compares the surface catalytic rate and analyte diffusion rate [(Chen *et al.* 2006)]. Recently, Pandey *et al*., developed an electrochemical sensor for Cys based PB nanocomposite and the results revealed the synergistic effect of AuNPs and nanostructured palladium on electrocatalysis [(Pandey *et al.* 2012)]. A

mechanistic approach study was done for the oxidation of N-acetyl-L-cysteine on the gold electrode [(Barus *et al.* 2007)] later N-acetyl-L-cysteine have been electrochemical detection was done by the active involvement of cobalt hexacyanoferrate or PB on the carbon paste modified electrode or on palladized aluminium electrode [(Heli *et al.* 2010; Pournaghi-Azar and Ahour 2008)]. Manganese hexacyanoferrate have also been used for the electrocatalytic oxidation of L-cysteine [(Wang *et al.*)]. In recent work, PB nanocomposite hybrid film anchored on graphene quantum dots modified graphite felt was used for the electrochemical detection of L-Cysteine [(Wang *et al.* 2016a)]. Many reports are available involving the MHCFs and its composite modified electrode electro oxidation of glutathione (GSH) sensing. Ravi Shankaran and Sriman Narayan, (2002), developed an amperometric sensor for GSH based on a mechanically immobilized cobalt hexacyanoferrate and copper hexacyanoferrate modified electrodes [(Ravi Shankaran and Sriman Narayanan 2002)]. The modified electrodes facilitates the catalytic oxidation of GSH at a reduced over potential and at the border pH range. Palladized aluminium electrode covered by PB film for electrocatalytic oxidation of GSH was developed by Pournaghi-Azar and Ahour, (2008); and the results show that metallic palladium layer inserted between PB film and Al which acts as an electron-transfer bridge [(Pournaghi-Azar and Ahour 2008)]. A kinetic study of the electrocatalytic oxidation of reduced glutathione at PB film modified electrode was done by Senthil Kumar using rotating-disc electrode voltammetry [(Kumar and Pillai 2009)]. Carbon nanofibre-PDDA/PB nanocomposite film modified ITO electrode was developed by Muthurulan and Velmurugan, (2011), to analyze direct electrochemistry and electrocatalysis of reduced GSH [(Muthirulan and Velmurugan 2011)]. Recently, Pandey et.al, (2012), developed a sensor based on NiHCF-AuNPs nanocomposite for selective sensing of GSH and the results justified the role of AuNPs for facilitated electrochemical activity of NiHCF based system as a function of nanogeometry [(Pandey and Pandey 2012b)]. Adekunle *et.al.,* (2011), synthesized a hybrid composite material composed of PB/single walled carbon nanotubes and used as a electrode modifier for the development of nitrite sensor based on simple adsorption controlled electrode reaction [(Adekunle *et al.* 2011)]. Stable

cinder/PBAs was used for the electrochemical oxidation of nitrite [(Zen *et al.* 2001)]. Graphene nanosheets, carbon nanosphere on the chitosan coated PB composite material was used for the electrochemical oxidation of nitrite [(Cui *et al.* 2012)]. Here, graphene nanosheets/carbon nanosphere acted as mediator. The synergy effect of CS@PB nanoparticles and GNS-CNS justified the excellent electrochemical response for the nitrite detection in terms of high sensitivity, low detection limit and short response time. In very recent work, a novel PB, ionic liquid 1-butyl-3-methylimidazolium tetrafluoroborate and graphite felt (GF) nanocomposite material was successfully used for the electrocatalytic determination of nitrite [(Wang *et al.* 2015)]. Adekunle *et.al*., (2012), developed a dopamine (DA) sensor based on electrocatalytic properties of PBNPs supported on poly (m-aminobenzenesulphonic acid)-sunctionalized single walled carbon nanotubes [(Adekunle *et al.* 2012)]. Hosseinzadeh *et al*., (2009) analyzed the effect of cetyltrimethylammonium bromide (CTAB) in determination of DA and ascorbic acid (AA) based on tin hexacyanoferrate modified carbon paste electrode and the justified that cationic surfactant, CTAB enables the separation of the oxidation peaks potential of DA and AA [(Hosseinzadeh *et al.* 2009)]. Another PB based modified electrode was used for the electrochemical oxidation study of dopamine by using hybrid inorganic-organic coating on platinum electrode [(Lupu *et al.* 2009)]. Copper-cobalt hexacyanoferrate has been used for the development of sensor for tryptophan determination [(Liu and Xu 2007)]. Prabhu *et.al*. (2011), made CuHCF/AuNPs film modified graphite-wax (GW) electrode for the quantitative determination of L-tryptophan (L-Trp) at a reduced overpotential of 400 mV [(Prabhu *et al.* 2011)]. In a simple method, electrodeposited PB has been used for the determination of sulphite [(García *et al.* 2005)]. Alamo *et al*., developed CuHCF-carbon nanotube modified carbon paste electrode for the determination of sulphite by pervaporation-flow injection method [(Alamo *et al.* 2010)]. Recently, a graphene/CuHCF nanocomposite was used for the amperometric sensing of captopril [(Gholivand *et al.* 2013)]. Studies showed that the combination of graphene and CuHCF significantly improve the current response of the GCE in the oxidation of captopril. PB/multiwalled carbon

nanotubes were used for the fabrication of electrochemical sensor for hydroxylamine [(Zhang *et al.* 2010a)].

1.2.1.2 Electrochemical sensor for non-electroactive species

The zeolytic nature of PB and its metal hexacyanoferrate have given the opportunity to explore its usability in the potentiometric and voltammetric sensors for electro inactive cations. These cations participate in the redox reactions of PB and its metal hexacyanoferrate property of which can be utilize for the development of sensors for these cations. Sensors based on these cations are either potentiometric or voltammetric. In PB, the channel radius was found to the order of 0.16 μm which can be occupied by hydrated ions like K^+, Rb^+, Cs^+ and NH_4^+ whose radius are found to the order of 0.125 μm, 0.128 μm, 0.119 μm and 0.125 μm respectively. The cations whose hydrated radii are larger than the channel radius of PB cannot intercalate through the PB crystal lattice like for example Li^+, Na^+, H^+, and all of the group II cations. The voltammetric investigation demonstrated that most suitable electrodes for determination of potassium ions are hexacyanoferrates of iron (III), copper (II), silver (I), nickel (II), and cadmium (II) while electrodes with nickel (II) and cadmium (II) hexacyanoferrates are suitable for caesium ion determination [(Düssel *et al.* 1996)]. Variation in PB for the detection of K^+ ions happens in various works like PB thin film [(Ho and Lin 2001)], PB nanotubes [(Nguyen *et al.* 2009)] and PB solid state films [(Krishnan *et al.* 1990)]. Apart of these potassium ion sensor, thallium and caesium ion sensor have also been developed by several groups [(Coon *et al.* 1998; Hartmann *et al.* 1991; Jain *et al.* 1982; Krishnan *et al.* 1990; Thomsen and Baldwin 1989; Zhiqiang *et al.* 1991)]. Recently, more analysis has been done with PB based material to investigate their ion-sieving capabilities. Cationic surfactant, CTAB modified PB electrode was fabricated and exploited to analyze the cation transport characteristics for K^+, Na^+, Li^+ and NH_4^+ ions [(Vittal *et al.* 2008)]. Nguyen *et.al*., (2009) reported PB nanotube sensor for Na^+ ions based on the inhibitory effect of Na^+ and K^+ inter/deintercalation [(Nguyen *et al.* 2009)]. An approach for dual sensing of Na^+ and K^+ ions using PB nanotubes through selective inter/deintercalation of K^+ and competitive inhibition by Na^+ ion was reported by

[(Ang *et al.* 2011)]. On 3rd October 2003, Food and Drug Administration (FDA), approved that 500 mg PB capsules can be utilized as a safe and effective drug for the treatment of contamination of radioactive caesium and radioactive thallium or non radioactive thallium. PB drug, known as Radiogardase, is used to trap the caesium or thallium in the gastrointestinal tract.

1.2.1.3 PB and its metal analogues based electrochemical biosensor

A biosensor is an analytical device used for the detection of analytes (living system or incorporating biological elements) which contains the physicochemical elements. The biological elements like tissues, microorganisms, cell receptors like enzymes, antibodies, nucleic acid etc. or biologically derived material interacts or binds to the analyte. The performance of biosensor strongly depends upon the electron transfer between the biomolecules and the electrode. Therefore, the proper immobilization of the biomolecules/biological material on the electrode surface is the main important task in construction of biosensor. The immobilization strategy resolves the operational stability and long term use or reusability of biosensor. Since, H_2O_2 is present in many biological reactions as the main product of several oxidase enzymes and the monitoring of the H_2O_2 is the main parameters for analyzing the bioprocess. After discovery of properties of PB and its metal analogues, opened a door for the exploring the possibility of utilizing it in the construction of biosensors. As we know, PB is an efficient redox mediator for the selective detection of H_2O_2; this is extensively used in the construction of PB based biosensor. Karyakin *et al.*, (1994) demonstrated the first application of metal hexacyanoferrates for the development of biosensor [(Karyakin *et al.* 1994)]. In this work, electrode modification was done by immobilizing glucose oxidase on the top of the PB layer with the help of nafion membrane. Another approach for the development of PB based biosensor for the same group that involved enzyme immobilization through entrapment into PB film during deposition and also in the flow injection analysis [(Karyakin *et al.* 1995; Karyakin *et al.* 1996)]. Later, Jaffari and Turner group demonstrated the analytical performances of PB based biosensor for the determination of blood glucose [(Jaffari and Pickup 1996a)]. Recently, a number of articles published concerning

the use of PB based glucose biosensor [(Ahmadalinezhad *et al.* 2009; Chen *et al.* 2012b; Fu *et al.* 2011; Wang *et al.* 2011)]. After utilization of PB alone in the construction of biosensor, later along with the PB other materials were also used to construct PB composite material in the construction of biosensor like PB/polyaniline/glucose oxidase [(Garjonyte and Malinauskas 2000a)], polyaniline-PB/multiwalled carbon nanotube [(Zou *et al.* 2007)], polypyrrole/poly(o-phenylenediamine)/PB modified electrode [(Garjonyte and Malinauskas 2000b)], PB/chitosan [(Wang *et al.* 2009; Wang *et al.* 2003)], PB/sol-gel chitosan/silica hybrid [(Tan *et al.* 2005)], PB/chitosan/gold nanopartices [(Xue *et al.* 2006)], Chitosan/PB/multiwalled carbon nanotube/hollow PtCo nanochain [(Che *et al.* 2011)], PB/aminophenol film [(Pan *et al.* 2004)], PB/carbon nanotube hybrid [(Fu *et al.* 2011)], PBNPs/carbon nanotubes/poly(1,2-diaminobenzene) [(Zeng *et al.* 2008)], PB/grafted carbon nanotube/Poly(4-vinylpyridine) composite [(Li *et al.* 2007)] and poly(3,4-ethylenedioxythiophene)/PB bilayer/ multiwalled carbon nanotube [(Chiu *et al.* 2009)] and many more is adding in this list. Not only glucose and H_2O_2 other analytes were also used for the development of PB based biosensor like cholesterol [(Li *et al.* 2003; Vidal *et al.* 2004)], ethanol [(Karyakin *et al.* 1996)], glutamate [(Wang *et al.* 2003)], lactate [(Salazar *et al.* 2012)], NADH [(Gurban *et al.* 2008)], organophosphorus pesticide [(Zhang *et al.* 2012a)] and uric acid [(Piermarini *et al.* 2013)]. This could be achieved by immobilizing different oxidase enzymes in selective layer of PB or in combination of other material as composite. As we know, change in oxidation state of PB is accompanied by a colour change. This property has been utilized for the construction of an optical biosensor. In this optical biosensor, PB film was chemically deposited on the non-conducting surface in polypyrrole network and utilized for ascorbic acid sensing which involve the change of the PB film absorbance as a function of analyte concentration [(Koncki and Wolfbeis 1998a, b)]. In another work for the development of glucose biosensor by the same group, glucose oxidase was immobilized onto Prussian White colourless film which oxidised in the presence of H_2O_2 produced by the enzymatic reaction to give a change in absorbance at 720 nm [(Koncki *et al.* 2001b; Lenarczuk *et al.* 2001b)]. In line of this, Lenarczuk et.al., (2001) explored the optical sensing activity of PB

based material for pharmaceutical applications [(Lenarczuk *et al.* 2001a)]. In a recent work, PB/chitosan modified graphene paste was used for the development of development of DNA biosensor in which graphene enhanced the sensitivity compare to graphite and chitosan protected the stability of PB film [(Bo *et al.* 2011)].

1.2.1.4 Advance transducer for H_2O_2 sensing

H_2O_2 shows both oxidizing and reducing properties which is a by-product of many oxidase enzyme catalyzed reactions. The analysis of as generated H_2O_2 has been used in the development of electrochemical sensor/biosensor. Initially, direct electrochemistry of H_2O_2 has been exploited because such analyte normally do not undergo mediated electrochemical reaction with redox mediators having well defined electrochemical behaviour. Direct electrochemistry of H_2O_2 occurs at relatively higher over-potential and accordingly subsequently efforts have been done on the use of electro catalytic material for hydrogen peroxide sensing. After the initial reports by Itaya and co-workers, the first report to analyze PB as electrochemical mediator for hydrogen peroxide was done by Boyer et.al. [(Boyer *et al.* 1990)]. Electrochemical oxidation of H_2O_2 triggers at anodic potentials (> +0.6V *vs*. Ag|AgCl) therefore the selective detection of H_2O_2 at low applied potential was thoroughly investigated by Karyakin group [(Karyakin *et al.* 1994; Karyakin *et al.* 1995; Karyakin *et al.* 1996)]. They claimed that the electrocatalytic activity of PB towards H_2O_2 was about 100 times greater than that of oxygen and the rate constant was estimated to be 5 x 10^2 $M^{-1}s^{-1}$. After the study of electrocatalytic oxidation of H_2O_2, electrocatalytic reduction of the same was studied by PB. The use of PB modified electrodes at an applied potential of 0.0 V *vs.* Ag|AgCl with sensitivity in the micromolar range facilitates selective and sensitive detection of PB [(Karyakin *et al.* 1996)]. The kinetics of PB catalyzed H_2O_2 reduction was found to be $3x10^3$ $M^{-1}s^{-1}$ under optimized condition, which is comparable to that measured for the peroxidise enzyme ($2x\ 10^4$ $M^{-1}s^{-1}$) [(Dunford and Hasinoff 1970)]. The operating potential 0.0 V was low enough to minimize the effect of many common electrochemical interfering materials. Because of both high activity and selectivity, PB was designated as artificial peroxidase [(Karyakin

and Karyakina 1999b; Karyakin *et al.* 2000; Lu *et al.* 2006)]. After that several articles have come up with the modification in either electrode or immobilization method of PB or in combination with PB for the detection of H_2O_2 [(Chi and Dong 1995; Dostal *et al.* 1995; Moscone *et al.* 2001; Ricci and Palleschi 2005)]. After utilization of PB as a sole material in the detection of H_2O_2, other material in combination of PB have used for the detection of H_2O_2 to increase the sensitivity and selectivity of the sensor. For example: self-assembled PB on glassy carbon electrode [(Liu *et al.* 2009)], chitosan-functionalized graphene nanosheets [(Yang *et al.* 2012)], carbon nanotube/poly(4-vinylpyridine) composite [(Li *et al.* 2007)], Rhodium-PB [(Ivama and Serrano 2003)], graphene oxide/PB [(Zhang *et al.* 2011b)], multiwalled carbon nanotubes, gold-chitosan colloid [(Li *et al.* 2009)], graphene [(Mao *et al.* 2011)], methylene blue/ silicon oxide nanocomposite [(Yao *et al.* 2005)], PB/multiwalled carbon nanotube [(Farah *et al.* 2012)], polypyrrole/PB nanowire [(Lin *et al.* 2011b)], PB@Pt nanoparticles/carbon nanotubes composite [(Zhang *et al.* 2009)], multiwalled carbon nanotubes/polypyrrole/PB composite [(Jin *et al.* 2012)] and thionine functionalized multiwalled carbon nanotubes [(Jeykumari *et al.* 2007)] and many more is adding in this. Not only PB, other metal hexacyanoferrate have also been used for the cathodic detection of H_2O_2 like cobalt (II) hexacyanoferrate [(Lin and Jan 1997)], chromium (III) hexacyanoferrate (II) [(Lin and Tseng 1998)], ruthenium oxide hexacyanoferrate [(Paixão and Bertotti 2008a)], palladium hexacyanoferrate [(Iveković *et al.* 2004)], vanadium hexacyanoferrate [(Tsiafoulis *et al.* 2005)], nickel hexacyanoferrate [(Fiorito and de Torresi 2005; Lin *et al.* 2005)] and gallium hexacyanoferrate [(Yu *et al.* 2007b)].

1.2.2 Artificial Peroxidase like activity of nanomaterial: Special reference to Prussian blue and its analogues in application of H_2O_2

Natural enzymes are the biological catalysts which have been used in a specific reaction and protein in nature. Natural enzymes have been used in clinical diagnosis, biotechnology, chemistry, environmental science and other fields of interests. Enzymes catalyzed reactions have high specificity, high efficiency under optimum conditions. In spite of these excellent properties, enzymes have some

drawbacks like (i) enzymes are very susceptible to the environmental conditions because their catalytic efficiency specifically depends upon the native protein conformations, (ii) Since enzymes are proteinaceous in nature so they can be easily digested in the presence of protease enzymes, (iii) Isolation and purification of enzymes are difficult, costly and time consuming. Therefore, a lot of efforts have been given to explore a material which works as an enzyme and also overcome these problems. In line of this, several efforts have been made in creating an alternative to natural enzymes cyctochrome P, hemin, hematin, porphyrin, cyclodextrin, dendrimers, polymers and many more [(Sono *et al.* 1996; Wang *et al.* 2007a; Wulff and Sarhan 1972; Zhang *et al.* 2004; Zhang *et al.* 2012c)].

The material which are not enzymatic in nature and works as enzymes are called Artificial enzymes, the term coined by Ronald Breslow for enzyme mimics [(Breslow and Overman 1970)]. Nanomaterial based artificial enzymes have also termed as "nanozymes" by Wei and Wang [(Wei and Wang 2013)]. In recent years, due to tremendous exploration in the field of nanoscience, some nanoparticles have shown the enzyme-like activity. Recently, novel finding proved that inorganic nanoparticles (Fe_3O_4) possess intrinsic peroxidase like activity and revealed the possibility to use as peroxidase replacement [(Gao *et al.* 2007)]. This surprising discovery has opened the door for the development of nanosized material for the use in the biochemical assay. After that, a variety of metal and carbon based nanomaterial have been reported as a enzyme mimics. For example: silver nanoparticles [(Jiang *et al.* 2012)], Au@Pt nanoparticles [(He *et al.* 2011)], bismuth-gold nanoparticles [(Lien *et al.* 2012)], Pd@Au nanoparticles [(Nangia *et al.* 2012)], cerium oxide nanoparticles [(Korsvik *et al.* 2007)], V_2O_5 nanowire [(André *et al.* 2011)], Co_3O_4 nanoparticles [(Yin *et al.* 2012)], carbon based material like graphene oxide [(Song *et al.* 2010a)], single walled carbon nanotubes [(Song *et al.* 2010b)], helical carbon nanotubes [(Cui *et al.* 2011)]. The inorganic nanomaterial are very interesting as they have better properties comparing to natural enzymes as they are more resistant to pH, temperature, large surface-to-volume ratio and resistant to protease digestion. In addition to that, their synthesis is cost effective and easy to prepare and store [(Asati *et al.* 2009; Chen *et al.*

2012a; Wang *et al.* 2012)]. Like other nanomaterial, PB based material have also been explored for the peroxidase like activity towards the oxidation of a variety of peroxidase substrate. Peroxidase-like activity of PB modified iron oxide magnetic nanoparticles was investigated by [(Zhang *et al.* 2010b)]. The calculated kinetic parameters exhibited strong affinity with substrate and high catalytic activity which are three orders of magnitude larger than that of the magnetic nanoparticles of similar size. PB modified Fe_2O_3 have shown the superior catalytic activity towards oxidation of peroxidase substrate 3,3'-5,5'-tetramethybenzidine (TMB) as peroxidase mimetic [(Dutta *et al.* 2012b)]. PB modified ferritin nanoparticles (Ft NPs) acted as peroxidase mimetic and also used for the detection of glucose detection [(Zhang *et al.* 2013)]. This Ft NPs were also utilized as a probe with the simultaneous combination of the peroxidase-like activity in immunosorbent assay. Recently, it was reported that PBNPs acted as peroxidase mimetic by using peroxidase substrate 2,2'-azino-bis(3-ethyl-benzothiazoline-6-sulfonic acid) diammonium salt [(Zhang *et al.* 2014)]. Multiwalled carbon nanotube was filled with PB and successfully utilized for the colorimetric detection of H_2O_2 and glucose by using tetramethylbenzidine (TMB) as a substrate [(Wang *et al.* 2014)].

Detection of H_2O_2 as peroxidase mimetic is done by catalyzing the conversion of different chromogenic substrates such as tetramethylbenzidine (TMB), o-phenylenediamine (OPD), o-dianisidine, or di-azo-aminobenzene (DAB) into coloured product using H_2O_2 as oxidizing agent [(Josephy *et al.* 1982; Ma *et al.* 2011)]. Similarly, in glucose detection technique, horseradish peroxidase (HRP) is used to catalyze reaction between chromogenic substrate and H_2O_2 which generates from glucose –glucose oxidase system. As generated H_2O_2 estimates by use of any of the above chromogenic substrates. However, this method has a major drawback by using HRP, natural enzymes, which easily denatured and loss its activity by slight environmental changes. Therefore, it is necessary to remove HRP by artificial enzyme to overcome a number of drawbacks. To achieve this objective, PB, its mixed metal analogues and composite material with PB may fulfil this requirement.

1.3 Challenges in Prussian blue and its mixed metal analogues related work

The possibility of huge application of PB and its mixed metal analogues have directed the researchers to search new synthetic route required for meeting the development of PB-based designs. The PB synthesis by conventional method has following drawbacks that limit the practical applicability.

1. The conventional method of synthesis of PB and its metal analogues involves direct mixing of Fe^{3+} or bivalent transition metal ions and $[Fe(CN)_6]^{4-}$ under stirring condition that leads to the uncontrolled growth of solid precipitate due to uncontrolled nucleation.
2. The insolubility of PB and its mixed metal analogues in common solvents are major problem that hinders the usability of PB and its analogues for practical applications.
3. Stability of PB and its mixed metal analogues suspension as a function of time is another drawback for potential applications. PB gets precipitated over the time.
4. Functionality in the PB and its metal analogues is a setback that restricts its application for various practical purposes in designing the practical devices. Functionalize the material with the biocompatible material may be helpful in the designing the biosensor.
5. The requirement of controlling the stoichiometric ratio of two metals in the three dimensional network may increase the possibility of getting better crystalline material for specific applications.

Accordingly, subsequent development have been made on the synthesis of PBNPs and mixed metal analogues by applying various approaches. The use of polymer, graphene or other material have been demonstrated on these lines [(Gotoh *et al.* 2007; Hu *et al.* 2012a; Jia 2011a; Qian *et al.* 2013; Yamada *et al.* 2009; Zhai *et al.* 2008)]. However, synthesis of biocompatible PB and its metal analogues nanoparticles which can be dispersed into a suitable solvent creating nanodispersion may leads to the development of PB based device and require a systematic investigation on the synthesis of PB and mixed metal analogues.

In addition to that, it is essential to explore the electrocatalytic applications of PB and its mixed metal analogues for practical purposes. It is also need to analyze the effect of stoichiometric effect of ratio of two different transition metal ions which may alter the electrocatalytic properties of its mixed metal analogues and effect of presence of other transition metal ions on the catalytic efficiency according to that of their differential redox activity, and the last one is the analytical performances of mixed metal analogues.

1.4 Origin of the present research work

Earlier studies conducted in our laboratory have shown the role of functionalized silanes on the formation of thin film of organically modified silicate (ormosil) demonstrating its role in the construction of electrochemical sensor. During this work, ion-exchange and ion recognising sites (Nafion, crown ether) have also been incorporated to alter the electrochemical behaviour of ormosil-encapsulated mediators. The resulting ormosil modified electrodes retain the inherent property of these organic moieties and have significantly increased the sensitivity for the analytes. Later on, potassium ferricyanide has been incorporated into the ormosil film along with such organic moiety and redox electrocatalysis during electrochemical sensing was realized. While incorporating dibenzo-18-crown-6 along with potassium ferricyanide into the ormosil film, the presence of tetrahydrofuran/cyclohexanone as a solvent in the ormosil precursors *i.e;* 3-aminopropyltrimethoxysilane (3-APTMS) and 2-(3,4-epoxycyclohexyl)ethyl trimethoxysilane), remarkable findings on the conversion of single precursor into Prussian blue was realized [(Pandey and Upadhyay 2005; Pandey *et al.* 2004)]. These finding directed for detailed investigation on the cyclohexanone and 3-APTMS mediated controlled synthesis of Prussian blue nanoparticles and its mixed metal analogues nanoparticles from single precursor $K_3[Fe(CN)_6]$ [(Pandey and Pandey 2013a, c, d)]. The as made PBNPs exhibited excellent electrochemistry with electronic transfer rate constant with the order of 32.1 s^{-1} [(Pandey and Pandey 2013c)]. In addition to that, the similar process also enabled the controlled synthesis of mixed metal hexacyanoferrates [(Pandey and Pandey 2013a, d)]. The disadvantage of the process is limited to use of 3-APTMS that

underwent hydrolysis, condensation and polycondensation thus affecting the properties of PBNPs for many practical applications. Fortunately, our group succeeded to replace 3-APTMS and cyclohexanone through the use of tetrahydrofuran-hydroperoxide (THF-HP) which efficiently allowed to converts potassium ferricyanide into water soluble, stable PBNPs in overnight time at room temperature. Poor commercial availability of THF-HPO and requirement of THF and peroxide components directed us to understand the role of tetrahydrofuran (THF) and hydrogen peroxide (H_2O_2) that may allow the synthesis of PBNPs. In addition to that choice of the other organic reducing agents like polyethylenimine (PEI) facilitating the crystalline behaviour of PB and its mixed metal analogues has also been one of the prime attentions of the present research program.

1.5 Objective of the present research work

As discussed in preceding sections, all the oxidase catalyzed reactions allow the formation of hydrogen peroxide based on following reaction Scheme.1.1.

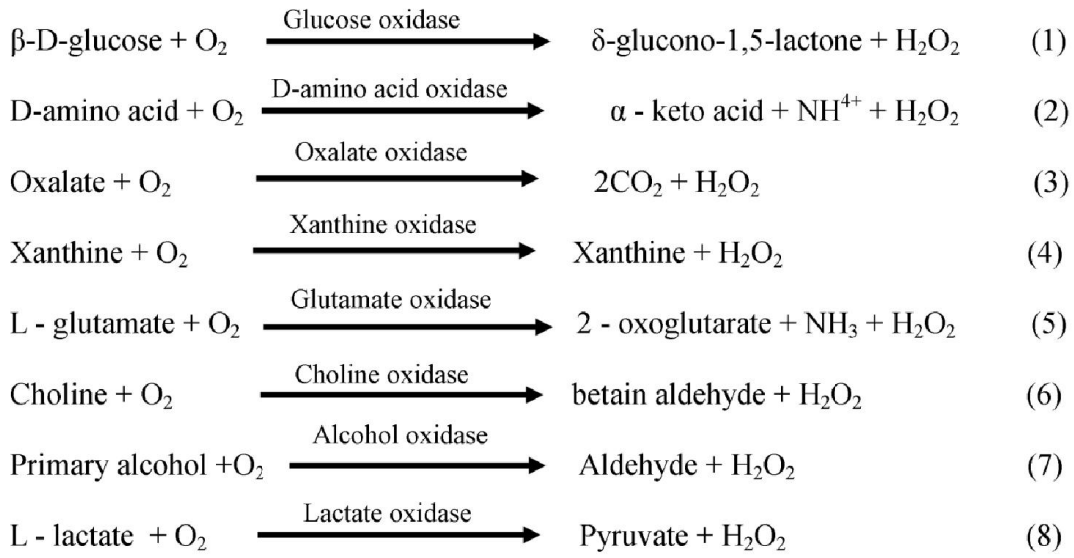

Scheme.1. 1. Examples of oxidase catalyzed reactions.

Scheme-1.1.depict the production of molecular oxygen during the course of all oxidases catalyzed reactions. Accordingly, the probing of these enzyme catalyzed reactions requires sensitive assays of as generated H_2O_2 during the course the enzymatic reactions. These enzymatic reactions have been frequently

used in sensitive clinical assays and play crucial role in controlling the healthcare problems. For example: clinical assay of blood glucose in clinical pathological laboratory explored the participation on GOD/POD system base on following reaction Scheme.1.2.

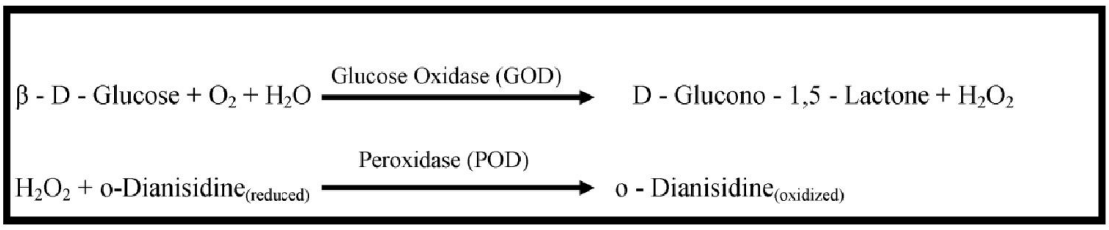

Scheme.1. 2. Reactions involved in GOD/POD system during pathological detection of blood glucose.

Scheme-1.2 depict the glucose was catalyzed by the presence of glucose oxidase and generate hydrogen peroxide as a by product could be detected in the presence of peroxidase enzyme and an organic dye named o-dianisidine or similarly others. The use of Peroxidase enzyme in the above reactions encounters the several problems because of poor stability of peroxidase which is susceptible for inactivation under different environmental conditions. Accordingly, there is a need to replace the use of peroxidase by suitable synthetic material having catalytic activity similar to that of peroxidase with biocompatibility for probing the oxidase catalyzed reactions by spectroscopy which has been an important requirement in clinical assay. Further, H_2O_2 can also be precisely detected through electrochemical oxidation and reduction of the same at the modified electrode surface. Accordingly, there is a need for development of novel nanomaterial that can be probed for H_2O_2 sensing by both spectroscopy and electrochemistry. Since, PB is referred as an artificial peroxidase, the design and development of processable Prussian blue which can be used in both spectrophotometrically and electrochemical detection of H_2O_2 has been one of the important requirements in analytical chemistry. Accordingly, the present research program is aimed on the development of processable Prussian blue which can be used for both spectrophotometrically and electrochemical detection of H_2O_2 generated during the enzymatic reaction and the research finding on the these lines on the synthesis

of processable Prussian blue is reported. Further the finding discussed in preceding section justify the role of suitable reagent that allow the control nucleation of Prussian blue leading to the formation of processable PBNPs for meeting the above requirement which has been the prime attention of the present thesis programme.

Therefore, the choice of organic reducing agents to control the nucleation during the synthesis of PB and its mixed metal analogues has been the prime attention of present thesis program. Accordingly, the findings on the following points constitute the major objectives for systematic investigations on following points:

1) Synthesis of Prussian blue using tetrahydrofuran and hydrogen peroxide and single precursor potassium ferricyanide that enables the solubility, functionality and nanogeometry.
2) Synthesis of mixed metal hexacyanoferrates using tetrahydrofuran, hydrogen peroxide, single precursor potassium ferricyanide and other transition metal ions.
3) Synthesis of Prussian blue mediated through polyethylenimine (PEI) to enhance biocompatibility and stability.
4) PEI mediated synthesis of Cu-Fe HCFs and Ni-Fe HCFs.
5) Characterization of the above synthesized PBNPs and its mixed metal analogues nanoparticles through UV-Vis spectroscopy, FT-IR, XRD, EDS, SEM and TEM.
6) Application of PBNPs and its mixed metal analogues nanoparticles in the development of electrochemical sensor for biologically important analytes like H_2O_2, hydrazine and dopamine.
7) Studies on the peroxidase like activity of PBNPs and its mixed metal analogues nanoparticles and their application in H_2O_2 detection.

1.6 Work plan for the present research work

The work plan performed in the present thesis is as follows:

1) Synthesis of nanocrystalline PBNPs mediated through organic moiety tetrahydrofuran (THF), hydrogen peroxide H_2O_2 and single precursor $K_3[Fe(CN)_6]$.
2) Synthesis of nanocrystalline mixed metal hexacyanoferrate with a variety of transition metals by THF, H_2O_2 and single precursor $K_3[Fe(CN)_6]$.
3) Synthesis of nanocrystalline PBNPs mediated through single precursor $K_3[Fe(CN)_6]$, PEI and HCl.
4) PEI mediated synthesis of nanocrystalline mixed metal hexacyanoferrate through active involvement of $K_3[Fe(CN)_6]$ and other transition metal ions like nickel and copper.
5) Characterization of synthesized material of PBNPs and its mixed metal hexacyanoferrate through structural and electrochemical methods.
6) Development of amperometric sensor based on PBNPs and its mixed metal analogues for the various biological important analytes like H_2O_2, hydrazine, dopamine.
7) Investigation about the peroxidase mimetic activity of as synthesized PBNPs and their mixed metal analogues to evaluate their kinetic catalytic efficiency towards the determination of towards H_2O_2.